for the Promotion of AIDS Research from the Ministry of Health, Labour and Welfare, a Grant for Research for Health Sciences Focusing on Drug Innovation from the Japan Health Sciences Foundation and the Science and Technology Incubation Program in Advanced Regions from the Japan Science and Technology Agency.

References

[1] E. De Clercq, Antiretroviral drugs, Curr. Opin. Pharmacol. 10 (2010) 507–515.
[2] P. Dorr, M. Westby, S. Dobbs, P. Griffin, B. Irvine, M. Macartney, J. Mori, G. Rickett, C. Smith-Burchnell, C. Napier, R. Webster, D. Armour, D. Price, B. Stammen, A. Wood, M. Perros, Maraviroc (UK-427,857), a potent, orally bioavailable, and selective small-molecule inhibitor of chemokine receptor CCR5 with broad-spectrum anti-human immunodeficiency virus type 1 activity, Antimicrob. Agents Chemother. 49 (2005) 4721–4732.
[3] C.T. Wild, D.C. Shugars, T.K. Greenwell, C.B. McDanal, T.J. Matthews, Peptides corresponding to a predictive alpha-helical domain of human immunodeficiency virus type 1 gp41 are potent inhibitors of virus infection, Proc. Natl. Acad. Sci. USA 91 (1994) 9770–9774.
[4] G. Fatkenheuer, A.L. Pozniak, M.A. Johnson, A. Plettenberg, S. Staszewski, A.I. Hoepelman, M.S. Saag, F.D. Goebel, J.K. Rockstroh, B.J. Dezube, T.M. Jenkins, C. Medhurst, J.F. Sullivan, C. Ridgway, S. Abel, I.T. James, M. Youle, E. van der Ryst, Efficacy of short-term monotherapy with maraviroc, a new CCR5 antagonist, in patients infected with HIV-1, Nat. Med. 11 (2005) 1170–1172.
[5] J.P. Lalezari, K. Henry, M. O'Hearn, J.S. Montaner, P.J. Piliero, B. Trottier, S. Walmsley, C. Cohen, D.R. Kuritzkes, J.J. Eron Jr., J. Chung, R. DeMasi, L. Donatacci, C. Drobnes, J. Delehanty, M. Salgo, Enfuvirtide, an HIV-1 fusion inhibitor, for drug-resistant HIV infection in North and South America, N. Engl. J. Med. 348 (2003) 2175–2185.
[6] Y. Feng, C.C. Broder, P.E. Kennedy, E.A. Berger, HIV-1 entry cofactor: functional cDNA cloning of a seven-transmembrane, G protein-coupled receptor, Science 272 (1996) 872–877.
[7] H. Tamamura, A. Omagari, S. Oishi, T. Kanamoto, N. Yamamoto, S.C. Peiper, H. Nakashima, A. Otaka, N. Fujii, Pharmacophore identification of a specific CXCR4 inhibitor, T140, leads to development of effective anti-HIV agents with very high selectivity indexes, Bioorg. Med. Chem. Lett. 10 (2000) 2633–2637.
[8] H. Tamamura, Y. Xu, T. Hattori, X. Zhang, R. Arakaki, K. Kanbara, A. Omagari, A. Otaka, T. Ibuka, N. Yamamoto, H. Nakashima, N. Fujii, A low-molecular-weight inhibitor against the chemokine receptor CXCR4: a strong anti-HIV peptide T140, Biochem. Biophys. Res. Commun. 253 (1998) 877–882.
[9] N. Fujii, S. Oishi, K. Hiramatsu, T. Araki, S. Ueda, H. Tamamura, A. Otaka, S. Kusano, S. Terakubo, H. Nakashima, J.A. Broach, J.O. Trent, Z.X. Wang, S.C. Peiper, Molecular-size reduction of a potent CXCR4-chemokine antagonist using orthogonal combination of conformation- and sequence-based libraries, Angew. Chem. Int. Ed. Engl. 42 (2003) 3251–3253.
[10] H. Tamamura, K. Hiramatsu, M. Mizumoto, S. Ueda, S. Kusano, S. Terakubo, M. Akamatsu, N. Yamamoto, J.O. Trent, Z. Wang, S.C. Peiper, H. Nakashima, A. Otaka, N. Fujii, Enhancement of the T140-based pharmacophores leads to the development of more potent and bio-stable CXCR4 antagonists, Org. Biomol. Chem. 1 (2003) 3663–3669.
[11] J.P. Lalezari, K. Henry, M. O'Hearn, J.S. Montaner, P.J. Piliero, B. Trottier, S. Walmsley, C. Cohen, D.R. Kuritzkes, J.J. Eron, J. Chung, R. DeMasi, L. Donatacci, C. Drobnes, J. Delehanty, M. Salgo, T.S. Group, Enfuvirtide, an HIV-1 fusion inhibitor, for drug-resistant HIV infection in North and South America, N. Engl. J. Med. 348 (2003) 2175–2185.
[12] A. Lazzarin, B. Clotet, D. Cooper, J. Reynes, K. Arasteh, M. Nelson, C. Katlama, H.J. Stellbrink, J.F. Delfraissy, J. Lange, L. Huson, R. DeMasi, C. Wat, J. Delehanty, C. Drobnes, M. Salgo, T.S. Group, Efficacy of enfuvirtide in patients infected with drug-resistant HIV-1 in Europe and Australia, N. Engl. J. Med. 348 (2003) 2186–2195.
[13] B. Labrosse, L. Morand-Joubert, A. Goubard, S. Rochas, J.L. Labernardière, J. Pacanowski, J.L. Meynard, A.J. Hance, F. Clavel, F. Mammano, Role of the envelope genetic context in the development of enfuvirtide resistance in human immunodeficiency virus type 1-infected patients, J. Virol. 80 (2006) 8807–8819.
[14] E. Poveda, B. Rodés, C. Toro, L. Martín-Carbonero, J. Gonzalez-Lahoz, V. Soriano, Evolution of the gp41 env region in HIV-infected patients receiving T-20, a fusion inhibitor, AIDS 16 (2002) 1959–1961.
[15] B. Zöllner, H.H. Feucht, M. Schröter, P. Schäfer, A. Plettenberg, A. Stoehr, R. Laufs, Primary genotypic resistance of HIV-1 to the fusion inhibitor T-20 in long-term infected patients, AIDS 15 (2001) 935–936.
[16] S. Oishi, S. Ito, H. Nishikawa, K. Watanabe, M. Tanaka, H. Ohno, K. Izumi, Y. Sakagami, E. Kodama, M. Matsuoka, N. Fujii, Design of a novel HIV-1 fusion inhibitor that displays a minimal interface for binding affinity, J. Med. Chem. 51 (2008) 388–391.
[17] T. Naito, K. Izumi, E. Kodama, Y. Sakagami, K. Kajiwara, H. Nishikawa, K. Watanabe, S.G. Sarafianos, S. Oishi, N. Fujii, M. Matsuoka, SC29EK, a peptide fusion inhibitor with enhanced alpha-helicity, inhibits replication of human immunodeficiency virus type 1 mutants resistant to enfuvirtide, Antimicrob. Agents Chemother. 53 (2009) 1013–1018.
[18] H. Nishikawa, S. Oishi, M. Fujita, K. Watanabe, R. Tokiwa, H. Ohno, E. Kodama, K. Izumi, K. Kajiwara, T. Naitoh, M. Matsuoka, A. Otaka, N. Fujii, Identification of minimal sequence for HIV-1 fusion inhibitors, Bioorg. Med. Chem. 16 (2008) 9184–9187.
[19] K. Izumi, E. Kodama, K. Shimura, Y. Sakagami, K. Watanabe, S. Ito, T. Watabe, Y. Terakawa, H. Nishikawa, S.G. Sarafianos, K. Kitaura, S. Oishi, N. Fujii, M. Matsuoka, Design of peptide-based inhibitors for human immunodeficiency virus type 1 strains resistant to T-20, J. Biol. Chem. (2009) 4914–4920.
[20] D.K. Davison, R.J. Medinas, S.M. Mosier, T.S. Bowling, M.K. Delmedico, J.J. Dwyer, N. Cammack, M.L. Greenberg, New fusion inhibitor peptides, TRI-999 and TRI-1144, are potent inhibitors of enfuvirtide and T-1249 resistant isolates. in: Program and Abstracts of the 16 th International AIDS Conference, August 13 -18, 2006,Toronto, Canada, Abstract THPE0021.
[21] J.J. Dwyer, K.L. Wilson, D.K. Davison, S.A. Freel, J.E. Seedorff, S.A. Wring, N.A. Tvermoes, T.J. Matthews, M.L. Greenberg, M.K. Delmedico, Design of helical, oligomeric HIV-1 fusion inhibitor peptides with potent activity against enfuvirtide-resistant virus, Proc. Natl. Acad. Sci. USA 104 (2007) 12772–12777.
[22] E.N. Fung, Z. Cai, T.C. Burnette, A.K. Sinhababu, Simultaneous determination of Ziagen and its phosphorylated metabolites by ion-pairing high-performance liquid chromatography–tandem mass spectrometry, J. Chromatogr. B Biomed. Sci. Appl. 754 (2001) 285–295.
[23] Z. Cai, E.N. Fung, A.K. Sinhababu, Capillary electrophoresis-ion trap mass spectrometry analysis of Ziagen and its phosphorylated metabolites, Electrophoresis 24 (2003) 3160–3164.
[24] C. Goffinet, I. Allespach, O.T. Keppler, HIV-susceptible transgenic rats allow rapid preclinical testing of antiviral compounds targeting virus entry or reverse transcription, Proc. Natl. Acad. Sci. USA 104 (2007) 1015–1020.
[25] O.T. Keppler, F.J. Welte, T.A. Ngo, P.S. Chin, K.S. Patton, C.L. Tsou, N.W. Abbey, M.E. Sharkey, R.M. Grant, Y. You, J.D. Scarborough, W. Ellmeier, D.R. Littman, M. Stevenson, I.F. Charo, B.G. Herndier, R.F. Speck, M.A. Goldsmith, Progress toward a human CD4/CCR5 transgenic rat model for de novo infection by human immunodeficiency virus type 1, J. Exp. Med. 195 (2002) 719–736.
[26] R. Shibata, A. Adachi, SIV/HIV recombinants and their use in studying biological properties, AIDS Res. Hum. Retroviruses 8 (1992) 403–409.
[27] B. Chackerian, E.M. Long, P.A. Luciw, J. Overbaugh, Human immunodeficiency virus type 1 coreceptors participate in postentry stages in the virus replication cycle and function in simian immunodeficiency virus infection, J. Virol. 71 (1997) 3932–3939.
[28] J. Kimpton, M. Emerman, Detection of replication-competent and pseudotyped human immunodeficiency virus with a sensitive cell line on the basis of activation of an integrated beta-galactosidase gene, J. Virol. 66 (1992) 2232–2239.
[29] H. Deng, R. Liu, W. Ellmeier, S. Choe, D. Unutmaz, M. Burkhart, P. Di Marzio, S. Marmon, R.E. Sutton, C.M. Hill, C.B. Davis, S.C. Peiper, T.J. Schall, D.R. Littman, N.R. Landau, Identification of a major co-receptor for primary isolates of HIV-1, Nature 381 (1996) 661–666.
[30] E.I. Kodama, S. Kohgo, K. Kitano, H. Machida, H. Gatanaga, S. Shigeta, M. Matsuoka, H. Ohrui, H. Mitsuya, 4′-Ethynyl nucleoside analogs: potent inhibitors of multidrug-resistant human immunodeficiency virus variants *in vitro*, Antimicrob. Agents Chemother. 45 (2001) 1539–1546.
[31] D. Nameki, E. Kodama, M. Ikeuchi, N. Mabuchi, A. Otaka, H. Tamamura, M. Ohno, N. Fujii, M. Matsuoka, Mutations conferring resistance to human immunodeficiency virus type 1 fusion inhibitors are restricted by gp41 and Rev-responsive element functions, J. Virol. 79 (2005) 764–770.
[32] H. Tamamura, K. Hiramatsu, S. Ueda, Z. Wang, S. Kusano, S. Terakubo, J.O. Trent, S.C. Peiper, N. Yamamoto, H. Nakashima, A. Otaka, N. Fujii, Stereoselective synthesis of [L-Arg-L/D-3-(2-naphthyl)alanine]-type (E)-alkene dipeptide isosteres and its application to the synthesis and biological evaluation of pseudopeptide analogues of the CXCR4 antagonist FC131, J. Med. Chem. 48 (2005) 380–391.
[33] K.K. Van Rompay, Evaluation of antiretrovirals in animal models of HIV infection, Antiviral Res. 85 (2010) 159–175.
[34] K. Nishizawa, H. Nishiyama, Y. Matsui, T. Kobayashi, R. Saito, H. Kotani, H. Masutani, S. Oishi, Y. Toda, N. Fujii, J. Yodoi, O. Ogawa, Thioredoxin-interacting protein suppresses bladder carcinogenesis, Carcinogenesis 32 (2011) 1459–1466.
[35] T. Kitaori, H. Ito, E.M. Schwarz, R. Tsutsumi, H. Yoshitomi, S. Oishi, M. Nakano, N. Fujii, T. Nagasawa, T. Nakamura, Stromal cell-derived factor 1/CXCR4 signaling is critical for the recruitment of mesenchymal stem cells to the fracture site during skeletal repair in a mouse model, Arthritis Rheum. 60 (2009) 813–823.
[36] M.E. Kuipers, J.G. Huisman, P.J. Swart, M.P. de Béthune, R. Pauwels, H. Schuitemaker, E. De Clercq, D.K. Meijer, Mechanism of anti-HIV activity of negatively charged albumins: biomolecular interaction with the HIV-1 envelope protein gp120, J. Acquir. Immune Defic. Syndr. Hum. Retrovirol. 11 (1996) 419–429.
[37] F. Groot, T.B. Geijtenbeek, R.W. Sanders, C.E. Baldwin, M. Sanchez-Hernandez, R. Floris, Y. van Kooyk, E.C. de Jong, B. Berkhout, Lactoferrin prevents dendritic cell-mediated human immunodeficiency virus type 1 transmission by blocking the DC-SIGN–gp120 interaction, J. Virol. 79 (2005) 3009–3015.
[38] M.C. Harmsen, P.J. Swart, M.P. de Béthune, R. Pauwels, E. De Clercq, T.H. The, D.K. Meijer, Antiviral effects of plasma and milk proteins: lactoferrin shows potent activity against both human immunodeficiency virus and human cytomegalovirus replication *in vitro*, J. Infect. Dis. 172 (1995) 380–388.
[39] H. Drakesmith, A. Prentice, Viral infection and iron metabolism, Nat. Rev. Microbiol. 6 (2008) 541–552.

Supplemental Material can be found at:
http://www.jbc.org/content/suppl/2012/07/02/M112.351551.DC1.html

THE JOURNAL OF BIOLOGICAL CHEMISTRY VOL. 287, NO. 35, pp. 29988–29999, August 24, 2012
© 2012 by The American Society for Biochemistry and Molecular Biology, Inc. Published in the U.S.A.

HIV-1 Reverse Transcriptase (RT) Polymorphism 172K Suppresses the Effect of Clinically Relevant Drug Resistance Mutations to Both Nucleoside and Non-nucleoside RT Inhibitors*[S]

Received for publication, February 8, 2012, and in revised form, April 24, 2012 Published, JBC Papers in Press, July 2, 2012, DOI 10.1074/jbc.M112.351551

Atsuko Hachiya[‡§], Bruno Marchand[‡1], Karen A. Kirby[‡], Eleftherios Michailidis[‡], Xiongying Tu[¶], Krzysztof Palczewski[¶], Yee Tsuey Ong[‡], Zhe Li[‡‖], Daniel T. Griffin[‡], Matthew M. Schuckmann[‡], Junko Tanuma[§], Shinichi Oka[§], Kamalendra Singh[‡], Eiichi N. Kodama[**], and Stefan G. Sarafianos[‡‖2]

From the [‡]Christopher S. Bond Life Sciences Center, Department of Molecular Microbiology and Immunology, University of Missouri School of Medicine, Columbia, Missouri 65211, the [§]AIDS Clinical Center, National Center for Global Health and Medicine, Tokyo 162-8655, Japan, [¶]Case Western University, Cleveland, Ohio 44106, the [**]Division of Emerging Infectious Diseases, Tohoku University School of Medicine, Sendai 980-8575, Japan, and the [‖]Department of Biochemistry, University of Missouri, Columbia, Missouri 65211

Background: The effect of HIV polymorphisms in drug resistance is unknown.
Results: RT polymorphism 172K suppresses resistance to nucleoside (NRTIs) and non-nucleoside RT inhibitors (NNRTIs) by decreasing DNA binding and restoring NNRTI binding.
Conclusion: 172K is the first HIV polymorphism suppressing resistance to diverse inhibitors.
Significance: Results provide new insights into interactions between the polymerase active site and NNRTI-binding sites.

Polymorphisms have poorly understood effects on drug susceptibility and may affect the outcome of HIV treatment. We have discovered that an HIV-1 reverse transcriptase (RT) polymorphism (RT_{172K}) is present in clinical samples and in widely used laboratory strains (BH10), and it profoundly affects HIV-1 susceptibility to both nucleoside (NRTIs) and non-nucleoside RT inhibitors (NNRTIs) when combined with certain mutations. Polymorphism 172K significantly suppressed zidovudine resistance caused by excision (*e.g.* thymidine-associated mutations) and not by discrimination mechanism mutations (*e.g.* Q151M complex). Moreover, it attenuated resistance to nevirapine or efavirenz imparted by NNRTI mutations. Although 172K favored RT-DNA binding at an excisable pre-translocation conformation, it decreased excision by thymidine-associated mutation-containing RT. 172K affected DNA handling and decreased RT processivity without significantly affecting the k_{cat}/K_m values for dNTP. Surface plasmon resonance experiments revealed that RT_{172K} decreased DNA binding by increasing the dissociation rate. Hence, the increased zidovudine susceptibility of RT_{172K} results from its increased dissociation from the chain-terminated DNA and reduced primer unblocking. We solved a high resolution (2.15 Å) crystal structure of RT mutated at 172 and compared crystal structures of RT_{172R} and RT_{172K} bound to NNRTIs or DNA/dNTP. Our structural analyses highlight differences in the interactions between α-helix E (where 172 resides) and the active site β9-strand that involve the YMDD loop and the NNRTI binding pocket. Such changes may increase dissociation of DNA, thus suppressing excision-based NRTI resistance and also offset the effect of NNRTI resistance mutations thereby restoring NNRTI binding.

Human immunodeficiency virus type 1 (HIV-1) reverse transcriptase (RT) has been a major target of antiviral therapies. There are two classes of approved RT drugs as follows: nucleos(t)ide RT inhibitors (NRTI)[3] and non-nucleoside RT inhibitors (NNRTI). NRTIs are incorporated in the nascent DNA chain during reverse transcription and block further DNA synthesis by acting as chain terminators because they lack a 3′-hydroxyl group required for formation of a phosphodiester bond (1–3). NNRTIs are noncompetitive allosteric inhibitors that decrease the rate of nucleotide incorporation by binding to a hydrophobic pocket adjacent to the catalytic site (4–6).

* This work was supported, in whole or in part, by National Institutes of Health Research Grants AI094715, AI076119, AI079801, and AI074389 (to S. G. S.). This work was also supported by a grant for the promotion of AIDS research from the Ministry of Health, Labor, and Welfare (to E. K., A. H., and S. O.), by a grant for the Japan Initiative for Global Research Network on Infectious Diseases from the Ministry of Education, Culture, Sports, Science, and Technology (to J. T. and S. O.), and by a grant for Bilateral International Collaborative R&D Program from the Korea Food and Drug Administration and the Ministry of Knowledge and Economy (to S. G. S.).
[S] This article contains supplemental Figs. 1 and 2 and Tables 1–4.
The atomic coordinates and structure factors (code 4DG1) have been deposited in the Protein Data Bank, Research Collaboratory for Structural Bioinformatics, Rutgers University, New Brunswick, NJ (http://www.rcsb.org/).
[1] Recipient of an American Foundation for AIDS Research Mathilde Krim fellowship and a Canadian Institutes of Health Research fellowship.
[2] To whom correspondence should be addressed: 471d Christopher S. Bond Life Sciences Center, 1201 E. Rollins St., Columbia, MO 65211. Tel.: 573-882-4338; E-mail: sarafianoss@missouri.edu.

[3] The abbreviations used are: NRTI, nucleoside RT inhibitor; NNRTI, non-nucleoside RT inhibitor; TAM, thymidine-associated mutation; AZT, zidovudine; NVP, nevirapine; EFV, efavirenz; d4T, stavudine; ddI, didanosine; TDF, tenofovir; ABC, abacavir; AZT-MP, AZT-monophosphate; SPR, surface plasmon resonance; PDB, Protein Data Bank; BisTris, 2-[bis(2-hydroxyethyl)amino]-2-(hydroxymethyl)propane-1,3-diol; RTI, RT inhibitor; RVT, D-2′,3′-didehydro-2′,3′-dideoxy-5-fluorocytidine; TP, triphosphate; 3TC, lamivudine; T/P, template/primer.

There are two main mechanisms for resistance to NRTIs. In the first mechanism, RT preferentially decreases incorporation of NRTI-triphosphates (TPs), while retaining the ability to use natural nucleotide substrates. This type of resistance is typically imparted by mutations close to the nucleotide-binding site of RT. For instance, K65R, L74V, and Q151M decrease the incorporation rate of NRTI-TPs (7–10), whereas M184V sterically hinders productive binding of lamivudine (3TC)-TPs at the dNTP-binding site (11). The second mechanism of NRTI resistance involves unblocking of the NRTI-terminated primers by an excision activity that uses ATP (12–15). This excision activity is enhanced (12) in the presence of mutations such as M41L, D67N, K70R, L210W, T215Y/F, and K219Q/E (thymidine-associated mutations, TAMs), which are selected during zidovudine (AZT) or stavudine (d4T) therapy (16, 17). It has been reported by several groups, including ours, that other RT mutations located far from the polymerase active site at the connection subdomain (E312Q, G335C/D, N348I, A360I/V, V365I, and A376S) confer resistance to NRTIs and/or NNRTIs (18–25). It has been proposed that reduction of RNase H cleavage caused by connection subdomain mutations contributes to NRTI resistance by providing more time for RT to carry out excision and resume productive DNA synthesis (24–28).

There are several examples of RT mutations that cause resistance to one drug and affect the emergence of resistance mutations to another drug. For example, treatment of patients with AZT and 3TC combinations often results in the emergence of the 3TC resistance mutation M184V, but it also delays acquisition of TAMs (29, 30). In addition, appearance of the primary didanosine (ddI) resistance mutation L74V precludes AZT resistance conferred by TAMs (29, 31). Conversely, appearance of the first TAM (T215Y) during AZT and ddI combination therapy suppresses emergence of L74V (32). Tenofovir (TDF) resistance mutation K65R has a strong negative association with TAMs but not with other NRTI mutations, including Q151M complex (Q151Mc) (33). The bidirectional phenotypic antagonism between K65R and TAMs suppresses not only AZT resistance conferred by TAMs but also abacavir (ABC), ddI, and TDF resistance conferred by K65R (33, 34). Moreover, NNRTI resistance mutations L100I and Y181C are also antagonistic to AZT resistance by TAMs (32, 35, 36) because they reduce ATP-mediated unblocking of AZT-terminated primers (34, 35, 37–39). Such antagonistic interactions between resistance mutations impart significant clinical benefits. Hence, to optimize clinical decisions, it is very important to understand how mutations may affect the phenotype of known drug resistance mutations.

It is known that certain HIV-1 RT polymorphisms beyond the currently known canonical NRTI resistance mutations contribute to the evolution of NRTI resistance (40). Polymorphisms T39A, K43E/Q, K122E, E203K, and H208Y lead to TAM-1 (M41L/L210W/T215Y), whereas D218E leads to TAM-2 (D67N/K70R/T215F/K219Q). Moreover, an extensive cross-sectional study has demonstrated that some HIV-1 RT polymorphisms strongly correlate with virological failure of NRTI-based treatments (41).

Although codon 172 of HIV-1 RT is usually an arginine (172R), a lysine (172K) polymorphism is also found in clinical samples (up to 1.0%, as reported at the HIV Drug Resistance Database) and in the BH10 laboratory strain, which is very commonly used in drug resistance studies. This study uses virological, biochemical, and structural tools to reveal the effect of 172K on NRTI NNRTI. We report that 172K significantly suppresses resistance to both NRTIs and NNRTIs, and we propose specific biochemical mechanisms for these effects.

EXPERIMENTAL PROCEDURES

Antiviral Agents—AZT, d4T, and ddI were purchased from Sigma. 3TC and TDF were purchased from Moravek Biochemicals, Inc. (Brea, CA). ABC, nevirapine (NVP), and efavirenz (EFV) were provided by the AIDS Research and Reference Reagent Program (National Institutes of Health).

Cells and Viruses—COS-7 and MAGIC-5 cells (CCR5 transduced HeLa-CD4/LTR-β-gal cells) were maintained in Dulbecco's modified Eagle's medium supplemented with 10% fetal calf serum, 100 unit/ml penicillin, and 100 μg/ml streptomycin and used for transfection and antiviral assays, respectively, as described previously (42).

RT mutations were introduced by site-directed mutagenesis as described previously (20, 43). The pNL101 HIV-1 infectious clone was provided by Dr. K.-T. Jeang (National Institutes of Health, Bethesda) and used for generating recombinant HIV-1 clones. Wild-type HIV-1 (HIV-1_{WT}) was constructed by replacing the *pol*-coding region of pNL101 (nucleotides position; nucleotide 2006 of ApaI site to 5785 of SalI site of pNL101) with HIV-1 BH10 strain. We introduced a silent mutation at nucleotide 4232 (TTTAGA to TCTAGA) of the *pol*-coding region to generate a unique XbaI site. The desired mutations were introduced into the XmaI-XbaI region (1643 bp), which encodes nucleotides 2590–4232 of pNL101. This cassette was cloned into the respective sites of pBluescript vector (Stratagene) and introduced mutation(s) using an oligonucleotide-based site-directed mutagenesis method. After mutagenesis, the XmaI-XbaI cassettes were inserted back into pNL101 and confirmed by sequencing. Viral stocks were obtained by transfection of each molecular clone into COS-7 cells, harvested, and stored at −80 °C until use.

Drug Susceptibility Assays—Single replication cycle drug susceptibility assays were performed in triplicates using MAGIC-5 cells as described previously (42). Briefly, MAGIC-5 cells were infected with diluted virus stock at 100 blue forming units in the presence of increasing concentrations of RTIs, cultured for 48 h, fixed, and stained with 5-bromo-4-chloro-3-indolyl-D-galactopyranoside (X-gal). The stained cells were counted under a light microscope. The susceptibility of RTIs was calculated as the concentration that reduces blue forming units (infection) by 50% (50% effective concentration [EC_{50}]).

Enzymes and Nucleic Acid Substrates—Mutant RTs were generated through site-directed mutagenesis and replaced into the pRT dual vector using restriction sites PpuMI and SacI for the p51 subunit and SacII and AvrII for the p66 subunit. Heterodimeric HIV-1 RTs (p66 and p51) were expressed in *Escherichia coli,* BL21, and purified as described previously (44, 45).

For the primer extension and RT processivity assays we used an 18-nucleotide DNA primer fluorescently labeled with Cy3 at the 5′ end (P_{18long}; 5′-Cy3 GTC CCT GTT CGG GCG CCA-3′)

annealed to a 100-nucleotide DNA template (T_{100}; 5′-TAG TGT GTG CCC GTC TGT TGT GTG ACT CTG GTA ACT AGA GAT CCC TCA GAC CCT TTT AGT CAG TGT GGA AAA TCT CTA GCA GTG GCG CCC GAA CAG GGA C-3′) as described previously (44–46). For steady state kinetics, an 18-nucleotide DNA primer 5′-labeled with Cy3 (P_{18}; 5′-Cy3 GTC ACT GTT CGA GCA CCA-3′) annealed to a 31-nucleotide DNA template (T_{31}; 5′-CCA TAG ATA GCA TTG GTG CTC GAA CAG TGA C-3′). For the site-specific Fe^{2+} footprinting assay, we used a 30-nucleotide DNA primer (P_{30}; 5′-TCT ACA CTG ATT GTC ACT GTT CGA GCA CCA-3′) annealed to a 43-nucleotide DNA template 5′-labeled with Cy3 (T_{43}; 5′-Cy3 CCA TAG CTA GCT ATG GTG CTC GAA CAG TGA CAA TCA GTG TAG A-3′).

Primer Extension Assays—Primer extension assays were performed in the presence of AZT-TP or NVP as we described previously (44). Reactions contained 50 nM T_{100}/5′-Cy3-P_{18long} mixed with 120 nM RT (in experiments with AZT-TP) or 80 nM RT (in experiments with NVP) in a buffer containing 50 mM Tris-HCl, pH 7.8, and 50 mM NaCl, 1 μM of each dNTP, 0.5 mM EDTA, and varying concentrations of AZT-TP or NVP. In NVP-containing reactions, RT was preincubated with template/primer (T/P) and inhibitor at 37 °C for 5 min. DNA synthesis was initiated by the addition of 10 mM $MgCl_2$. Reactions were terminated after 40 min (AZT-TP) or 30 min (NVP) by adding an equal volume of 100% formamide-containing traces of bromphenol blue. Extension products were loaded on a 7 M urea, 15% polyacrylamide gel. The gels were scanned using a FLA-5000 PhosphorImager (FujiFilm, Stamford, CT). The amounts of full-length extended and unextended products were quantified by densitometry using MultiGauge, and the results were plotted using GraphPad Prism 4 (GraphPad Software Inc.).

Site-specific Fe^{2+} Footprinting Assays—Site-specific Fe^{2+} footprinting assays were performed using 5′-Cy3-labeled DNA templates as described previously (46, 47). Briefly, 100 nM 5′-Cy3-T_{43}/P_{30} was incubated at 37 °C with HIV-1 RT (600 nM) for 30 min in a buffer containing 120 mM sodium cacodylate, pH 7.0, 20 mM NaCl, 6 mM $MgCl_2$, and 10 μM AZT-TP to allow quantitative chain termination. Complexes were preincubated for 7 min with increasing concentrations of the next nucleotide (dATP), and 1 mM ammonium iron sulfate was added. The reactions were quenched after 5 min with 30 μl of formamide containing bromphenol blue. The products were resolved with gel electrophoresis in 7 M urea, 15% polyacrylamide gels.

Surface Plasmon Resonance Assay—We used surface plasmon resonance (SPR) to measure the binding affinity of RT_{172K} and RT_{172R} to double-stranded DNA. Experiments were performed on a Biacore T100 instrument (GE Healthcare). To prepare the sensor chip surface, we used the 5′-biotin-T_{d37}/P_{d25} (5′-biotin-TAG ATC AGT CAT GCT CCG CGC CCG AAC AGG GAC TGT G-3′, annealed to P_{d25} 5′-CAC AGT CCC TGT TCG GGC GCG GAG C-3′). Approximately 100 resonance units of this DNA duplex were bound in a channel of a streptavidin-coated sensor chips (Series S Sensor Chip SA) by flowing 0.1 μM DNA (flow rate 10 μl/min) in 50 mM Tris, pH 7.8, 50 mM NaCl. The binding constants were determined as follows: RT binding was observed by flowing solutions containing increasing concentrations of the enzyme (0.5, 1, 2, 4, 7.5, 10, 15, and 20 nM) in 50 mM Tris, pH 7.8, 60 mM KCl, 10 mM $MgCl_2$ in sample and background channels at 30 μl/min. The background traces were subtracted from the traces of the corresponding samples to obtain the binding signal of RT. This signal was analyzed using the Biacore T100 Evaluation software to determine K_D, k_{on}, and k_{off} values.

Enzyme Processivity Assays—Processivity assays were performed in the presence of a heparin trap to ensure that each synthesized DNA molecule resulted from a single processive cycle. Twenty nanomolar T_{100}/5′-Cy3-P_{18long} was preincubated with 500 nM RT at 37 °C in a buffer containing 50 mM Tris-HCl, pH 7.8, 50 mM NaCl, 50 μM of each dNTP, and 0.1 mM EDTA for 5 min. DNA synthesis was initiated by the addition of 10 mM $MgCl_2$ and 2 mg/ml heparin. Reactions were terminated after 0, 15, and 90 min by adding an equal volume of 100% formamide containing traces of bromphenol blue. Extension products were loaded on a 7 M urea, 15% polyacrylamide gel, quantified, and analyzed as described above.

Steady State Kinetics—Steady state parameters K_m and k_{cat} for incorporation of a nucleotide were determined using a single nucleotide incorporation gel-based assay. Reactions with RT_{172K} and RT_{172R} were carried out in 50 mM Tris-HCl, pH 7.8, 50 mM NaCl, 6 mM $MgCl_2$, 100 nM T/P, 10 nM RT, respectively, and varying concentrations of dNTP in a final volume of 10 μl. The reactions for HIV-1 RT were carried out in Reaction Buffer with 100 nM T_{31}/5′-Cy3-P_{18}. Reactions were stopped after 1 min at 37 °C, and the products were resolved and quantified as described above. K_m and k_{cat} values were determined graphically by using the Michaelis-Menten equation.

Crystallization of RT—RT with mutations K172A and K173A was prepared as described by Bauman *et al.* (48). These changes have been reported to strongly improve diffraction of RT. The enzyme was crystallized by the hanging drop vapor diffusion technique at 4 °C. The well solution contained 50 mM BisTris, pH 6.8, 100 mM ammonium sulfate, 10% glycerol, and 12% PEG 8000. Two μl of the well solution was mixed with 2 μl of RT (30 mg/ml) containing 10 mM $MgCl_2$, 10 mM Tris, pH 7.8, and 25 mM NaCl. The drop was equilibrated against the well solution by hanging a coverslip over the sealed well. The drops were streak-seeded with crushed RT crystals after 7 days of incubation. Crystals were obtained 7–14 days after the drops were seeded. Single crystals were soaked in cryoprotectant solution containing the well solution supplemented with 22.5% ethylene glycol for 15–60 s and frozen in liquid nitrogen.

Structure Solution—Diffraction datasets were collected at the Advanced Light Source Synchrotron beamline 4.2.2. The data were processed to 2.15 Å using MOSFLM (49) (supplemental Table 1). Molecular replacement phasing was performed using Phaser (50) and a previously solved RT structure as a model (Protein Data Bank (PDB) code 3KLI). The final model was obtained after cycles of iterative model building in COOT (51) and restrained refinement with CNS (52) and REFMAC (53). Final statistics for data processing and structure refinement are listed in supplemental Table 1. Coordinates and structure factors for the crystal structure were deposited to the PDB (PDB code 4DG1).

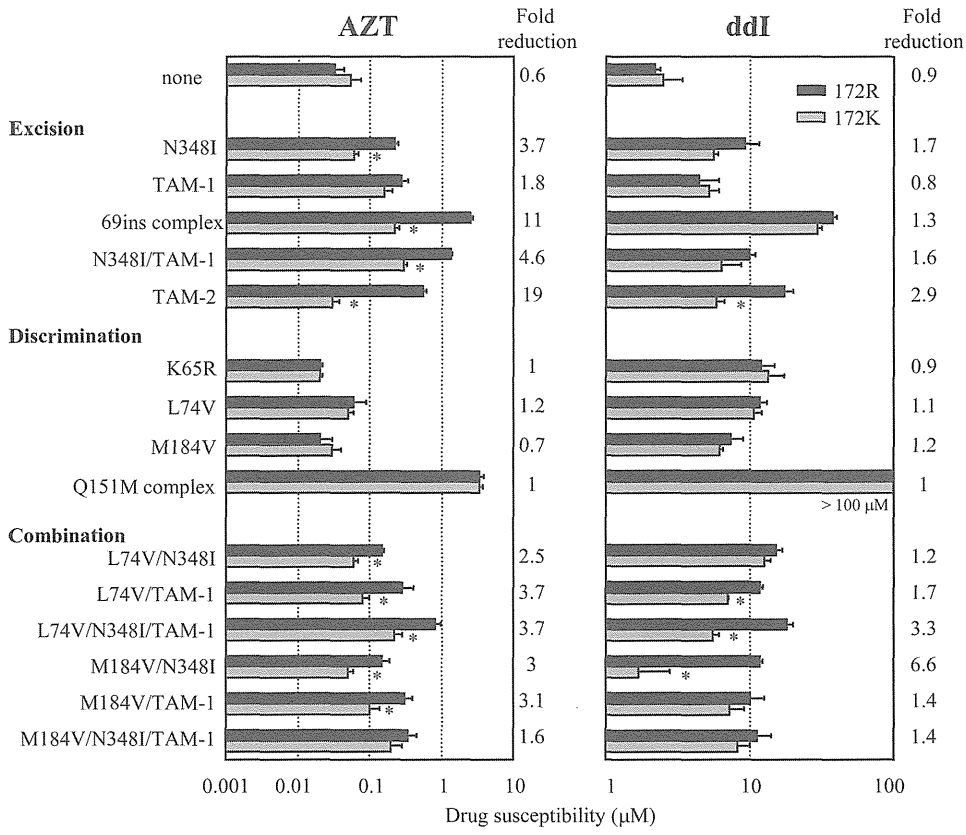

FIGURE 1. **Effect of the 172K polymorphism on HIV-1 susceptibility to AZT and ddI.** Antiviral activities of HIV-1 carrying NRTI resistance mutations with 172R (*black bars*) or 172K (*gray bars*) were determined by MAGIC-5 cell-based assay and shown as the concentration required for 50% inhibition of virus infection (EC_{50}). "TAM-1 and -2" have the "M41L and T215Y" and "D67N, K70R, T215F, and K219Q" mutations, respectively. 69ins complex carries 69 insertion and TAM-1. Q151Mc complex carries Q151M, A62V, V75I, F77L, and F116V. *Error bars* represent standard deviations from at least three independent experiments. *Asterisks* mark statistically significant differences ($p < 0.05$ by *t* test) in EC_{50} values comparing 172K with 172R in the background of NRTI-resistant mutations. Susceptibility of the Q151Mc complex with 172R or 172K to ddI was not assessed because the EC_{50} values were over the detection limit for this assay (>100 μM).

Structural Analysis—The program COOT was used to align crystal structure coordinates (typically using residues 107–112 and 151–215 of the p66 subunit) of the following complexes: RT_{172R} RT-EFV with RT_{172K} RT-EFV (PDB code numbers 1FK9 and 1IKW), $RT_{172R/K103N}$ RT-EFV with $RT_{172K/K103N}$ RT-EFV (PDB code numbers 1FKO and 1IKV), and RT_{172R} RT-NVP with RT_{172K} RT-U05 (a NVP analog) (PDB code numbers 1RTH and 3HVT). We also compared RT-DNA-dNTP ternary complexes (1RTD and 3JYT, as examples of RT_{172R} and RT_{172K} RTs). Figures were generated using PyMOL Molecular Graphics Program.

RESULTS

Effect of 172K on NRTI Resistance—To determine the effect of 172R or 172K on NRTI resistance, we generated RT_{172R} and RT_{172K} mutants carrying various NRTI-resistant mutations (Fig. 1 and supplemental Table 2) and compared the EC_{50} value of HIV-1_{172R} with that of HIV-1_{172K} in the background of NRTI-resistant mutations shown as a "fold reduction" in the Fig. 1. Although 172K alone had no effect on AZT or ddI susceptibility, 172K significantly reduced the AZT resistance of the following mutants that are associated with the excision mechanism: N348I, 69ins complex N348I/TAM-1 and TAM-2. Similarly, 172K appeared to suppress ddI resistance of a mutant that is associated with the excision mechanism TAM-2. In contrast, 172K had no statistically significant impact on AZT or ddI resistance of viruses with mutations that cause drug resistance by decreasing incorporation of NRTIs (K65R, L74V, M184V, and Q151Mc) (Fig. 1).

When we examined the effect of 172K on viruses that had combinations of mutations that cause NRTI resistance through the excision mechanism and through the decreased incorporation mechanism, we observed that 172K significantly suppressed resistance of L74V/TAM-1, L74V/N348I/TAM-1, and M184V/N348I, to AZT and to ddI (Fig. 1). These data suggested that 172K augments the suppressive effects of L74V and M184V on AZT and ddI resistance.

To further examine the effect of 172K on resistance to other Food and Drug Administration-approved NRTIs, we focused on the susceptibility of the 69ins complex to d4T, ABC, TDF, and 3TC (Table 1). Our data show that the 172K polymorphism significantly suppressed resistance of the 69ins complex to d4T (3-fold reduction; Table 1) and to AZT (11-fold reduction; Fig. 1). However, the resistance of 69ins complex to 3TC (54), ABC, and TDF was not significantly affected by 172K (less than 1.2-fold reduction in resistance). These results indicate that the suppressive effect of 172K can be NRTI-specific.

Effect of 172K on NNRTI Resistance—The antagonistic effects of 172K on the NNRTI resistance of RTs with mutations at K103N, V106M, V108I, Y181C, Y188L, and N348I are shown in Fig. 2 (and also supplemental Table 3). Fold reduction was

TABLE 1

Antiviral activities of NRTIs against HIV-1 encoding 69ins complex mutations in the background of 172K or 172R polymorphisms

Mutation(s)	EC_{50} (μM) (fold increase)[a]			
	d4T	ABC	TDF	3TC
172R	2.8 ± 0.9	2.7 ± 0.3	0.03 ± 0.01	1.5 ± 0.5
69ins complex/172R	16.7 ± 1.5 (6)	38.7 ± 3.1 (14)	0.16 ± 0.01 (5)	16.0 ± 1.0 (11)
69ins complex/172K	5.5 ± 1.3 (2)[b]	35.7 ± 2.5 (13)	0.13 ± 0.03 (4)	14.0 ± 1.0 (9)

[a] Values are means from at least three independent experiments, and the relative increase in the EC_{50} value for recombinant viruses compared with 172R is shown in parentheses.

[b] EC_{50} of 69ins complex with 172K is significantly different from that with 172R ($p < 0.0006$ by t test).

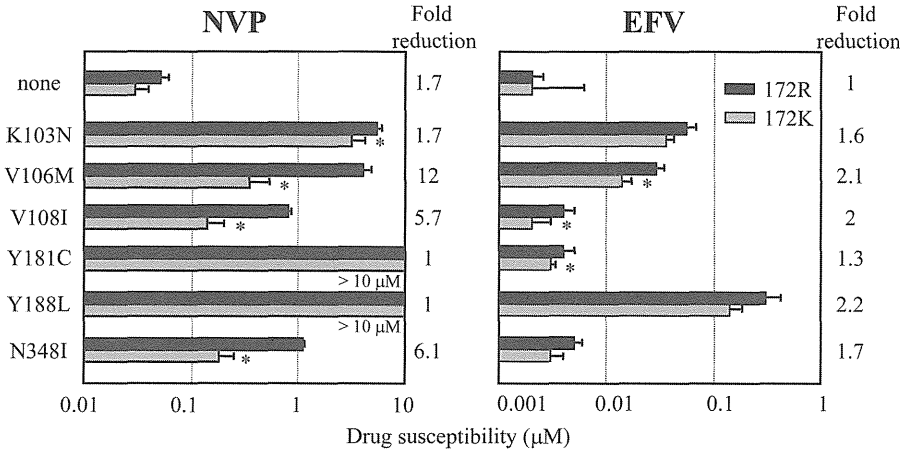

FIGURE 2. **Effect of the 172 polymorphism on HIV-1 susceptibility to NVP and EFV.** Antiviral activities of HIV-1 carrying NNRTI resistance mutations with 172R (*black bars*) or 172K (*gray bars*) were determined by MAGIC-5 cell-based assay and shown as the concentration required for 50% inhibition of virus infection (EC_{50}). *Error bars* represent standard deviations from at least three independent experiments. *Asterisks* mark statistically significant differences ($p < 0.05$ by t test) in EC_{50} values comparing 172K with 172R in the background of NNRTI-resistant mutations. Susceptibilities of Y181C or Y188L with 172R or 172K to NVP were not assessed because their EC_{50} values were over the detection limit for this assay (>10 μM).

TABLE 2

Primer extension assay of RT inhibition by AZT in the presence or absence of ATP

HIV-1 RT	IC_{50} of AZT-TP (nM)[a] (-fold increase)[b]		Excision enhancement by ATP[c]
	Without ATP	With ATP	
172R	286 ± 30 (1)	359 ± 18 (1)	1.3
172K	148 ± 5 (0.52)	183 ± 13 (0.52)	1.2
172R/TAM-2[d]	250 ± 20 (0.87)	995 ± 126 (2.78)	4.0
172K/TAM-2[d]	290 ± 19 (1.01)	517 ± 36 (1.44)	1.8

[a] The data are means ± S.D. from at least three independent experiments.

[b] Fold increase was compared with each WT 172R (without/with ATP).

[c] Excision enhancement by ATP is calculated as (IC_{50} with ATP)/(IC_{50} without ATP).

[d] TAM-2 carries D67N, K70R, T215F, and T219Q.

calculated as "EC_{50} of 172R/EC_{50} of 172K." 172K significantly suppressed NVP resistance conferred by K103N, V106M, V108I, and N348I. The impact of 172K on NVP resistance in the context of Y181C or Y188L could not be assessed, because both exhibited very high resistance (>10 μM) under these conditions. 172K also reduced EFV resistance of V106M, V108I, and Y181C. Hence, the impact of 172K on EFV resistance was considerably lower than that on NVP resistance. Collectively, our data demonstrate that RT resistance to NNRTIs (especially to NVP) can also be affected by 172K. A similar effect has been observed in assays using purified RTs containing either 172R or 172K. A lysine at position 172 conferred a higher susceptibility to NVP, while displaying only marginal differences for EFV, etravirine, and rilpivirine when compared with RT containing an arginine at that position (data not shown).

Effect of 172K on AZT Resistance of HIV-1 RT—TAMs cause AZT resistance by enhancing the ability of RT to remove the terminal AZT-monophosphate (AZT-MP) from the 3′-primer terminus using a pyrophosphate donor such as ATP. To determine whether 172K suppresses AZT resistance through a reduction in the efficiency of ATP-mediated excision, we purified RT_{172R} and RT_{172K} with TAM-2. We measured the susceptibility of RTs to inhibition by AZT in the presence or absence of ATP in a primer extension assay that uses long T/P (T_{100}/5′-Cy3-P_{18long}) (Table 2 and also supplemental Fig. 1). Any changes in AZT susceptibility *only* in the presence of ATP would suggest that the effect is excision-dependent. $RT_{172R/TAM-2}$ showed ~4-fold higher IC_{50} in the presence of ATP (995 *versus* 250 nM), although $RT_{172K/TAM-2}$ exhibited only a 1.8-fold excision enhancement by ATP (517 *versus* 290 nM). Hence, the ATP-based (or excision-based) increase in AZT resistance in TAM-2 was at least twice as much in the presence of 172R than 172K (4-fold *versus* 1.8-fold excision enhancement). However, in the absence of TAMs the effect of ATP was comparable for RT_{172R} and RT_{172K} (1.3-fold *versus* 1.2-fold excision enhancement) and smaller than in the case of the TAM enzymes. To further confirm these results, we also performed ATP-rescue assay using $RT_{172R/TAM-2}$

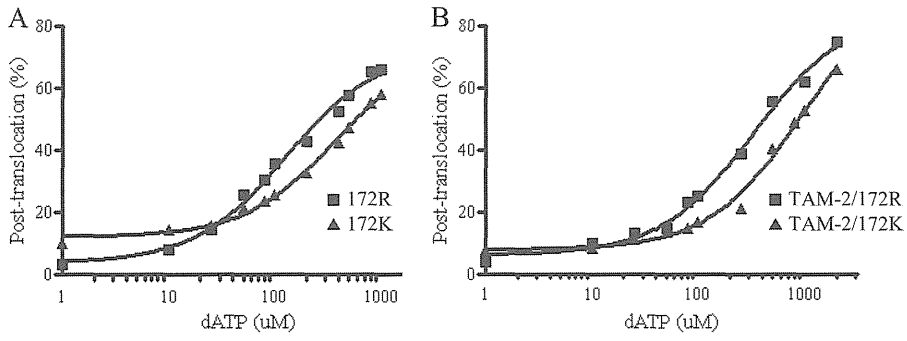

C

	172R	172K	TAM-2/172R	TAM-2/172K
Concentration of dATP needed to translocate 50% of RT / [μM]	128	388	327	940

FIGURE 3. **Effect of the 172 polymorphism on the translocation state of various HIV-1 RTs.** The effect of added dNTP on the translocation site of HIV-1 RT is compared for 172R (■) and 172K (▲) (*A*), as well as for TAM-2/172R (■) and TAM-2/172K (▲) (*B*). Complexes of RT with a double-stranded DNA terminated by a dideoxynucleotide were mixed with different concentrations of dATP eventually forming dead end complexes that position the nucleic acid in a post-translocation site. The dead end complexes were treated with hydroxyl radicals prepared in the presence of Fe^{2+}, and the nucleic acids were cleaved at position −18 or −17, depending on whether they were bound in a pre- or a post-translocation site. We quantified the bands in post- and pre-translocation sites and plotted the percent translocation. The concentrations of dATP required to translocate by 50% are shown in *C*.

and $RT_{172K/TAM\text{-}2}$. The rescue assays involve unblocking of AZT-terminated primers through ATP-based excision and DNA synthesis. $RT_{172K/TAM\text{-}2}$ also decreased ATP-excision reactions (data not shown). Hence, the suppressive effect of 172K in AZT resistance is ATP excision-dependent.

Effect of 172K on the Translocation Site of HIV-1 RT Measured by Fe^{2+} Footprinting—A single cycle of DNA polymerization involves dNTP binding, incorporation, and translocation of the elongated DNA primer from the dNTP-binding site (pre-translocation site, N-site) to the priming site (post-translocation site, P-site). For efficient ATP-based excision, the AZT-MP-terminated primer needs to be positioned at the pre-translocation site (14, 47). To determine whether 172K influences the positioning of AZT-MP-terminated primers, we performed a site-specific Fe^{2+} footprinting assay (Fig. 3). We mixed various RTs with AZT-terminated DNA and different concentrations of the incoming dATP substrate to form dead end complexes that position DNA in a post-translocation site. Treatment with hydroxyl radicals prepared in the presence of Fe^{2+} allowed cleavage at positions that correspond to pre- or post-translocation sites, and we monitored translocation as a function of dATP required to translocate 50% of RT. In this assay, lower numbers indicate more efficient translocation. Our data indicated that $RT_{172R/TAM\text{-}2}$ (or $RT_{172K/TAM\text{-}2}$) required higher dATP concentrations than RT_{172R} (or RT_{172K}) to translocate by 50% (327 *versus* 128 μM or 940 *versus* 388 μM). These data are consistent with previous reports that AZT-resistant RTs with excision mutations primarily bind in a pre-translocation site (47) and is thus more accessible for ATP-based excision. Interestingly, although $RT_{172K/TAM\text{-}2}$ has suppressed AZT resistance compared with $RT_{172R/TAM\text{-}2}$, it still bound the AZT-MP-terminated primer more efficiently in an excision-competent pre-translocation site (940/327 = 2.9-fold). Taken together, our data suggest that the decreased excision by 172K is *not* due to repositioning of the AZT-MP-terminated primer at the nonexcisable post-translocation site.

DNA Binding by HIV-1 RT Measured by Surface Plasmon Resonance—We hypothesized that the decreased excision-based resistance of 172K is due to a more efficient dissociation of the nucleic acid substrate, such that it decreases the opportunities to unblock chain terminated primers, thus resulting in suppression of AZT resistance. Hence, we used SPR to measure DNA binding and compare the DNA binding affinities of RT_{172K} and RT_{172R}. We chose SPR because measurements of the dissociation constant, $K_{D.\,DNA}$, using gel-mobility shift assays, do not offer insights regarding the kinetics of binding (k_{on}) and release (k_{off}) of nucleic acid from the enzyme. We attached biotinylated DNA on a streptavidin sensor chip and flowed various concentrations of either enzyme over the chip to measure the association (k_{on}) and dissociation (k_{off}) rates of the enzymes in real time (Fig. 4). The k_{off} value for RT_{172K} was markedly increased (31-fold) with a slightly changed k_{on} value (2.9-fold) compared with those for RT_{172R}. The $K_{D.\,DNA}$ ($=k_{off}/k_{on}$) value for RT_{172K} was 11-fold higher than that for RT_{172R} (1.8 and 0.16 nM, respectively). Our results demonstrate that RT_{172K} had lower DNA binding affinity than RT_{172R} due to a significant difference in the dissociation rate of RT from the DNA.

Processivity of HIV-1 RT—Considering that low DNA binding affinity by 172K may contribute to decreased processivity, we carried out processivity assays using RT_{172K} or RT_{172R} in the absence or presence of the NRTI resistance background. Assays were carried out using a long DNA template in the presence of heparin as a competitive trap (Fig. 5). Full-length product formation was less observed in RT_{172K} compared with RT_{172R}, indicating that 172K attenuates processivity. When introduced into $RT_{TAM\text{-}2}$, 172K lowered processivity even more. In contrast, Q151Mc may enhance RT processivity, as Q151Mc was more processive than WT, especially in the presence of RT_{172K}. These data suggest that 172K could decrease RT processivity in the background of only excision and not discrimination resistance mutations.

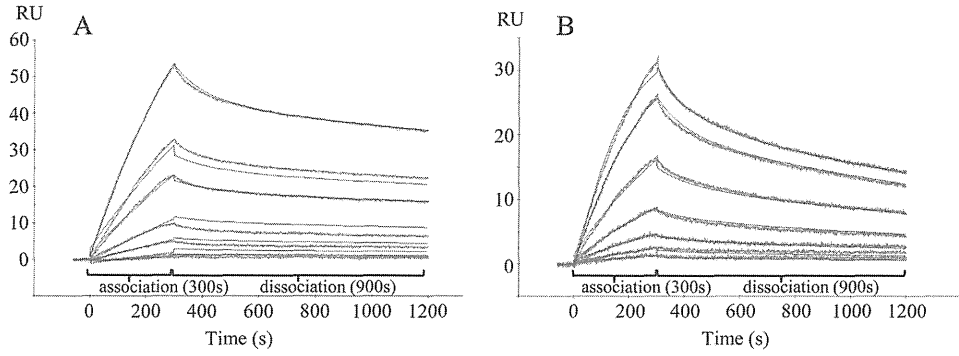

C

HIV-1 RT	K_d (nM)	k_{on} ($s^{-1}M^{-1}$)	k_{off} (s^{-1})
172R	0.16	8.3×10^4	1.4×10^{-5}
172K	1.8	2.4×10^5	4.3×10^{-4}

FIGURE 4. **Assessment of $K_{D.\ DNA}$, k_{on}, and k_{off} using SPR.** SPR was used to measure the DNA binding affinity of RTs with an arginine or a lysine at codon 172 (172R in *A* and 172K in *B*). Increasing concentrations (0.5, 1, 2, 4, 7.5, 10, 15, and 20 nM) of each RT were flowed over a streptavidin chip with biotinylated double-stranded DNA (5′-biotin-T_{d37}/P_{d25}) immobilized on its surface as described under "Experimental Procedures." The experimental trace (*red*) shown is the result of a subtraction of the data obtained from the channel containing the immobilized DNA minus the signal obtained from a control/background channel. DNA binding constants for RT_{172R} or RT_{172K} are shown in *C*.

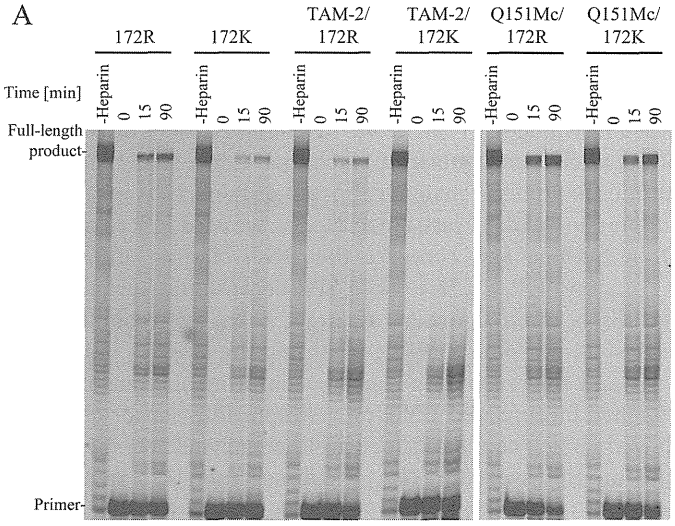

B

HIV-1 RT	Full-length DNA synthesis at 90 min (%)	
	172R	172K
none	8.4	3.2
TAM-2	3.5	0.2
Q151Mc	21.9	18.4

FIGURE 5. **Effect of changes at codon 172 on the processivity of HIV-1 RT.** *A*, processive DNA synthesis was measured at 0, 15, and 90 min after initiation of the reaction in the presence of heparin trap for each RT enzyme (WT, TAM-2, and Q151Mc) with 172R or 172K. Conditions were selected so that in the absence of heparin trap (*1st lane* of every set, labeled as *−Heparin*), the sum of processive and distributive DNA synthesis was the same (comparable full-length product in *−Heparin* lanes). All experiments were repeated three times and a representative gel is shown here. *B*, amount of full-length extended and un-extended products at 90 min after initiation of the reaction were quantified by densitometry using MultiGauge. Percentages of full-length DNA synthesis are shown in *B*.

TABLE 3
dATP incorporation under steady state conditions

HIV-1 RT	K_m	k_{cat}	k_{cat}/K_m
	nM	min^{-1}	$min^{-1} \cdot nM^{-1}$
172R	132	4.2	0.03
172K	143	7.2	0.05

TABLE 4
NVP susceptibility assay at the enzyme and virus level

Mutation	IC_{50} of NVP,[a] Enzyme (RT)[c]	EC_{50} of NVP,[a] HIV virus[b]
	nM	nM
172R	965 ± 55 (1)[b]	50 ± 10 (1)[b]
172K	174 ± 46 (0.2)[b]	30 ± 10 (0.6)[b]
172R/V106M	54795 ± 5565 (57)[b]	4100 ± 760 (83)[b]
172K/V106M	6181 ± 1096 (6)[b]	350 ± 190(7)[b]

[a] The data are means ± S.D. from at least three independent experiments.
[b] Fold increase was compared with WT 172R.
[c] These data were obtained from primer extension assay in the presence of NVP.
[d] These data were obtained from cell-based assay using MAGIC-5.

Steady State Kinetics of Nucleotide Incorporation—Initial polymerase activity comparisons of RT_{172R} and RT_{172K} showed that 172K slowed the polymerase activity of RT. This observation led us to investigate the steady state nucleotide incorporation properties of RT_{172R} and RT_{172K} using single nucleotide incorporation assays (Table 3). The estimated values for k_{cat} and $K_{m.dNTP}$ show that RT_{172K} and RT_{172R} had comparable efficacies ($k_{cat}/K_{m.dNTP}$ of 0.05 *versus* 0.03 min^{-1} nM^{-1}) under steady state conditions. These data suggested that 172K decreased RT processivity without affecting catalytic efficiency for nucleotide incorporation.

Susceptibility of HIV-1 RT to NVP—To examine the suppressive effect of 172K on NNRTI resistance at the HIV-1 RT enzyme level, we purified HIV-1 RT with V106M in the background of Arg or Lys at RT codon 172 and performed primer extension assays in the presence of NVP (Table 4). When introduced into RT_{V106M}, 172R results in an enzyme ($RT_{172R/V106M}$) with 57-fold resistance to NVP. In contrast, $RT_{172K/V106M}$ showed decreased resistance to NVP (6-fold). Hence, the extent of the suppressive effect of 172K on NVP resistance at the enzyme level was comparable with the effect observed at the virus level.

Crystal Structure of HIV-1 RT with Mutation at Codon 172—The structure of RT with the K172A mutation was determined at 2.15 Å resolution (supplemental Table 1). This is one of the

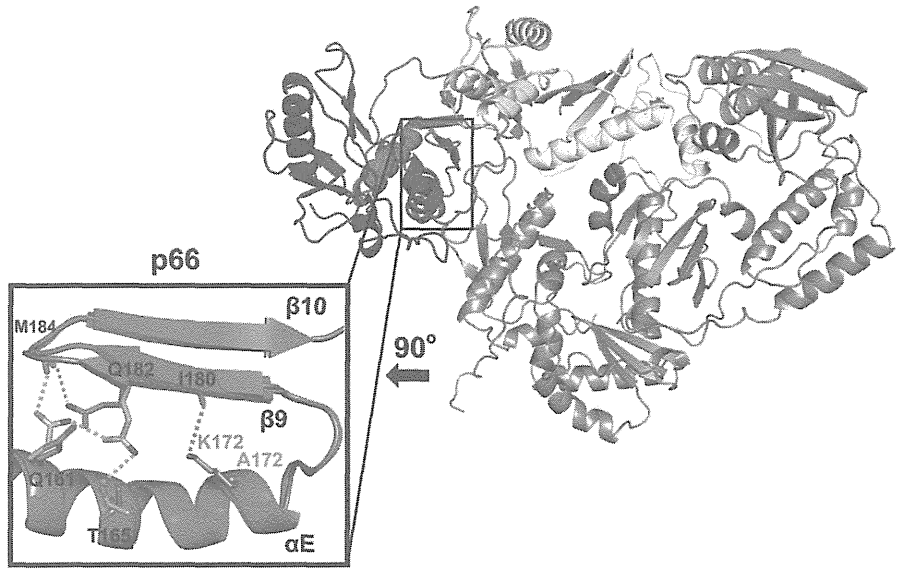

FIGURE 6. **Structural comparison of unliganded HIV-1 RT structures with Lys or Ala at codon 172.** HIV-1 RT with 172 mutated to alanine (PDB code 4DG1) is shown superposed to HIV-1 RT containing a 172K (PDB code 1DLO). Noticeable changes are observed in the hydrogen bond network between residues from α-helix E (161, 165, and 172) and from β9-strand (180, 182, and 184). The p66 palm subdomains of RT containing 172K or 172A are shown in *light blue* and *red*, respectively.

highest resolution structures of HIV-1 RT. In addition to this mutation, RT had also the K173A mutation to improve the crystallographic properties of the enzyme (48). However, we confirmed K173A did not affect susceptibility of RT to NVP and AZT, and it also did not alter the effect of the 172R or 172K change to susceptibility to RTIs at the virus or at the enzyme level (data not shown). The overall conformation of the mutant RT is similar to that of WT unliganded RT in which the p66 thumb subdomain is folded down into the DNA binding cleft (55). However, there are notable changes proximal to mutated residue 172 of the α-helix E, which affect interactions with residues of the β9-strand that leads to the YMDD loop of the polymerase active site. The Lys-172–Ile-180 interaction is lost in the 172A structure. This change is accompanied by a repositioning of the amide side chain of Gln-182, which in the 172K structure stabilizes the Met-184 main chain amide of the YMDD loop, whereas in the 172A structure it makes hydrogen bonds with the Thr-165 hydroxyl group and the Gln-161 side chain amide. Hence, the changes in the interactions between 172 and 180 propagate toward the polymerase active site (Fig. 6).

Effect of 172K on the Structure of HIV-1 RT—To further examine how 172K can simultaneously decrease to both NRTI and NNRTI resistances, we performed structural comparisons by aligning the crystal structures of RT_{172R} and RT_{172K} RTs in complex with NNRTIs. Interestingly, the structural changes observed among RT complexes that have different amino acids at position 172 follow the same pattern, albeit with small variations, as we observed in the comparisons among the unliganded structures (see above). In all cases, 172K and 172R of the α-helix E interact differently with residue 180 of the β9-strand, and this change affects in turn interactions between other residues of these structural elements as follows: 161 and 165 of the α-helix E, with 182 and 184 of the β9-strand (Fig. 7). Specifically, the RT_{172R} structure in complex with NVP shows that 172R and Gln-161 in α-helix E interact with Ile-180 and Gln-182 and indirectly with Met-184 in the β9-strand (Fig. 7*A*). The RT_{172R} structure in complex with EFV also shows that the 172R side chain contacts Ile-180 and has an additional interaction with Gln-182 through a water molecule (Fig. 7*B*). The RT_{172R} complex with EFV also shows that α-helix E helps stabilize β9-strand by a hydrogen bond between Thr-165 and Gln-182. In contrast, RT_{172K} in complex with NVP analog U05 has no interactions with Ile-180, Met-184, and Gln-161, following repositioning of surrounding residues (Fig. 7*A*). Similarly, RT_{172K} in complex with EFV shows loss of interactions of Ile-180 and Thr-165, but additional interactions are gained through Gln-161 with both Met-184 and Gln-182 (Fig. 7*B*). This loss of interaction between 172K and Ile-180 and Gln-182 is also observed in the presence of nucleic acid substrate (Fig. 7*C*). Furthermore, in the reported crystal structure of $RT_{172R/K103N}$, the aromatic side chain of Tyr-181 seems to flip almost 90° in the opposite direction and is likely to affect NNRTI susceptibility (Fig. 7*D*). Taken together, this information suggests that the residues in α-helix E may be involved in stabilizing the β9-strand, which is a part of the polymerase active site where NRTIs bind and of the NNRTI binding pocket. Changes in the interactions between the residues of α-helix E and β9-strand may affect the positioning of the YMDD loop, thus affecting not only NRTI and NNRTI binding but also substrate or DNA binding. This is consistent with previous reports on reduction of RT processivity due to changes in the YMDD loop (56, 57).

DISCUSSION

Our virological and biochemical data demonstrate that 172K suppresses resistance to both NRTIs and NNRTIs. Moreover, we established that the suppression of NRTI resistance by 172K involves a decrease in ATP-mediated excision. Previous studies have demonstrated that some NRTI and NNRTI resistance mutations can also affect excision-based NRTI resistance.

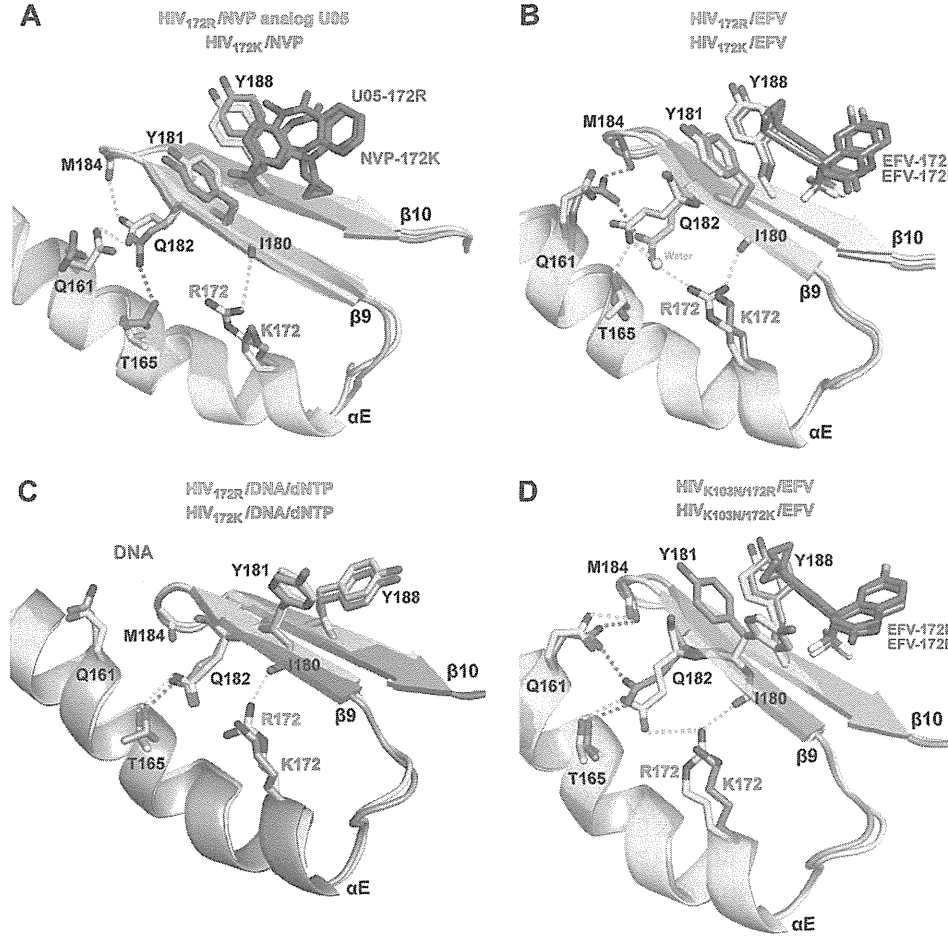

FIGURE 7. **Structural comparison of HIV-1 RT complexes with Lys or Arg at codon 172.** *A*, comparison of RT_{172R} (*cyan* side chains and *ribbons*) bound to NVP analog U05 (*blue sticks*) *versus* RT_{172K} (*pink side chains* and *ribbons*) bound to NVP (*pink sticks*). The change of 172R (*cyan*) to 172K (*pink*) affects the interactions between side chains of β-9–10 sheet and α-helix E. *B*, comparison of RT_{172R} (*cyan* side chains and *ribbons*) bound to EFV (*blue sticks*) *versus* RT_{172K} (*pink* side chains and *ribbons*) bound to EFV (*red sticks*). Similarly to *A*, the 172K → 172R change affects the intermolecular interactions between side chains of β-9–10 sheet and α-helix E. *C*, comparison of RT_{172R} (*cyan* side chains and *ribbons*) and RT_{172K} (*pink* side chains and *ribbons*) complexes with DNA and dNTP (not shown). *D*, comparison of $RT_{K103N/172R}$ (*cyan* side chains and *ribbons*) bound to EFV (*blue sticks*), and $RT_{K103N/172K}$ (*pink* side chains and *ribbons*) bound to EFV (*red sticks*). In addition to changes in the interactions between side chains of β-9–10 sheet and α-helix E also observed in *A* and *B*, the side chain of Tyr-181 "flips" in the 172K *versus* the 172R structure.

Hence, NRTI resistance mutations K65R, K70E, L74V, and M184V and NNRTI resistance mutations L100I and Y181C block ATP-mediated excision and suppress AZT resistance (32–35, 37, 38). In contrast, other NRTI resistance mutations (V118I and T215Y) impart NNRTI hyper-susceptibility to HIV-1 (58). To our knowledge, 172K is the first polymorphism that suppresses resistance to two independent types of inhibitors, NRTIs and NNRTIs.

Pathak and co-workers (24–27) proposed that connection subdomain mutations enhance NRTI and NNRTI resistance by reducing RNase H activity, thereby providing additional time for RT to bind in an NRTI excision-competent mode or allow NNRTIs to dissociate from RT (RNase H-dependent resistance mechanism). It is likely that connection subdomain mutations can also cause RNase H-independent AZT resistance. For example, mutation G333D does not reduce RNase H function, but it increases ATP-mediated excision, likely the result of long range interactions (27, 59). In addition, N348I confers NRTI and NNRTI resistance and increases ATP-mediated excision of AZT by both RNase H-dependent and independent mechanisms (60). The antagonistic effects of Y181C or M184V on phenotypic AZT resistance cannot be counteracted by N348I (19, 61). Interestingly, 172K reduces the resistance (to NRTIs or NNRTIs) that N348I imparts to HIV when added to WT, L74V, L74V/TAM-1, M184V, or M184V/TAM-1 backgrounds (Fig. 1). We showed that 172K can either slightly increase (RT_{172K} *versus* RT_{172R}) or decrease ($RT_{172K/TAM-2}$ *versus* $RT_{172R/TAM-2}$) the RNase H activity (supplemental Fig. 2). Hence, 172K does not have a consistent effect on RNase H function and is thus unlikely to reduce NRTI or NNRTI resistance by restoring the RNase H defect introduced by N348I.

How then is 172K reducing NRTI resistance? There are several possible mechanisms by which a residue could enhance susceptibility to NRTIs. First, it could improve NRTI incorporation into DNA. However, this is not the case with 172K because the IC_{50} values for AZT inhibition of $RT_{172R/TAM-2}$ or $RT_{172K/TAM-2}$ are not significantly different under conditions where only incorporation and not excision are examined (in the absence of ATP) (Table 2 and also supplemental Fig. 1). Second, a residue could increase sensitivity to NRTIs by decreasing excision. This could be accomplished by several ways including the following: (*a*) by promoting translocation of the NRTI-ter-

minated primer to the post-translocation site (47), which is not accessible to ATP, thus preventing NRTI excision (47). This is also not the case with 172K, as RT_{172K} favors the pre-translocated mode of binding (Fig. 3), which allows unblocking of chain-terminated primers; (*b*) by decreasing the excision efficiency through impaired use of the excision substrate ATP. However, our data (not shown) do not support this possibility, as we do not find any significant difference in ATP binding between $RT_{172R/TAM-2}$ and $RT_{172K/TAM-2}$ or RT_{172R} and RT_{172K} (the apparent K_m for ATP in a rescue-type assay for all enzymes is ~3 mM); (*c*) by increasing the dissociation of chain-terminated T/P, thereby limiting unblocking. Our data are consistent with this apparently novel mechanism of suppression of NRTI resistance. Specifically, SPR measurements indicate that RT_{172K} had decreased affinity for nucleic acid due to an increased dissociation rate (Fig. 4) (k_{off} was ~31-fold higher in the case of RT_{172K}). Hence, our data suggest that RT_{172K} has decreased AZT resistance primarily because the AZT-terminated template/primer falls off of the enzyme and cannot be unblocked. This is also consistent with the observed decrease in processivity of RT_{172K} and $RT_{172K/TAM-2}$ (Fig. 5). Interestingly, the processivity of $RT_{172K/Q151Mc}$ was not reduced (Fig. 5). Hence, it is possible that the relatively higher prevalence of $RT_{172K/Q151Mc}$ (9.9%, supplemental Table 4) compared with $RT_{172K/TAM-2}$ is likely due to the higher processivity and presumably higher fitness of $RT_{172K/Q151Mc}$.

The structural basis of decreased NNRTI resistance and AZT excision by RT_{172K} is likely related to how changes at 172 affect the positioning and mobility of the active site YMDD loop during the course of polymerization. The structural analysis of the crystal structures solved here and previously (Figs. 6 and 7) predict some changes in the interactions of the β9-strand with the α-helix E. The changes are propagated toward the polymerase active site and may affect the relative motions of the YMDD loop during the course of polymerization. Our previously published work has established that the mobility of YMDD is important for NRTI excision, processivity (57), and NNRTI susceptibility (56). Hence, it is possible that 172K affects NRTI and NNRTI resistance by changing the local environment of YMDD.

The R172K change emerges during serial passages of HIV-1 in MT-2 cells in increasing concentrations of Reverset (RVT, D-2′,3′-didehydro-2′,3′-dideoxy-5-fluorocytidine), a nucleoside analog with potent activity against HBV and AZT-resistant HIV-1, especially in the presence of TAMs (62, 63). Phenotypic analysis revealed that K70N/V90I/R172K had a 3.9-fold increase in RVT resistance (64). Our findings indicate that appearance of 172K during RVT therapy may also affect resistance to other drugs and should be taken into consideration in designing RVT-based therapeutic strategies.

In conclusion, we have identified the first RT polymorphism that suppresses resistance to both NRTIs and NNRTIs. The effect of polymorphisms in suppressing NRTI and NNRTI resistance provides new information into the interactions between the polymerase active site and the NNRTI-binding site of RT. These findings provide valuable insights for the design of antiviral regimens and new RT inhibitors.

REFERENCES

1. Mitsuya, H., Yarchoan, R., and Broder, S. (1990) Molecular targets for AIDS therapy. *Science* **249,** 1533–1544
2. Furman, P. A., Fyfe, J. A., St Clair, M. H., Weinhold, K., Rideout, J. L., Freeman, G. A., Lehrman, S. N., Bolognesi, D. P., Broder, S., Mitsuya, H., *et al.* (1986) Phosphorylation of 3′-azido-3′-deoxythymidine and selective interaction of the 5′-triphosphate with human immunodeficiency virus reverse transcriptase. *Proc. Natl. Acad. Sci. U.S.A.* **83,** 8333–8337
3. Singh, K., Marchand, B., Kirby, K. A., Michailidis, E., and Sarafianos, S. G. (2010) Structural aspects of drug resistance and inhibition of HIV-1 reverse transcriptase. *Viruses* **2,** 606–638
4. Sarafianos, S. G., Marchand, B., Das, K., Himmel, D. M., Parniak, M. A., Hughes, S. H., and Arnold, E. (2009) Structure and function of HIV-1 reverse transcriptase. Molecular mechanisms of polymerization and inhibition. *J. Mol. Biol.* **385,** 693–713
5. de Clercq, E. (1996) Non-nucleoside reverse transcriptase inhibitors (NNRTIs) for the treatment of human immunodeficiency virus type 1 (HIV-1) infections. Strategies to overcome drug resistance development. *Med. Res. Rev.* **16,** 125–157
6. Spence, R. A., Kati, W. M., Anderson, K. S., and Johnson, K. A. (1995) Mechanism of inhibition of HIV-1 reverse transcriptase by non-nucleoside inhibitors. *Science* **267,** 988–993
7. Deval, J., Selmi, B., Boretto, J., Egloff, M. P., Guerreiro, C., Sarfati, S., and Canard, B. (2002) The molecular mechanism of multidrug resistance by the Q151M human immunodeficiency virus type 1 reverse transcriptase and its suppression using α-boranophosphate nucleotide analogs. *J. Biol. Chem.* **277,** 42097–42104
8. Deval, J., Navarro, J. M., Selmi, B., Courcambeck, J., Boretto, J., Halfon, P., Garrido-Urbani, S., Sire, J., and Canard, B. (2004) A loss of viral replicative capacity correlates with altered DNA polymerization kinetics by the human immunodeficiency virus reverse transcriptase bearing the K65R and L74V dideoxynucleoside resistance substitutions. *J. Biol. Chem.* **279,** 25489–25496
9. Huang, H., Chopra, R., Verdine, G. L., and Harrison, S. C. (1998) Structure of a covalently trapped catalytic complex of HIV-1 reverse transcriptase. Implications for drug resistance. *Science* **282,** 1669–1675
10. Sarafianos, S. G., Pandey, V. N., Kaushik, N., and Modak, M. J. (1995) Glutamine 151 participates in the substrate dNTP binding function of HIV-1 reverse transcriptase. *Biochemistry* **34,** 7207–7216
11. Sarafianos, S. G., Das, K., Clark, A. D., Jr., Ding, J., Boyer, P. L., Hughes, S. H., and Arnold, E. (1999) Lamivudine (3TC) resistance in HIV-1 reverse transcriptase involves steric hindrance with β-branched amino acids. *Proc. Natl. Acad. Sci. U.S.A.* **96,** 10027–10032
12. Boyer, P. L., Sarafianos, S. G., Arnold, E., and Hughes, S. H. (2001) Selective excision of AZTMP by drug-resistant human immunodeficiency virus reverse transcriptase. *J. Virol.* **75,** 4832–4842
13. Meyer, P. R., Matsuura, S. E., So, A. G., and Scott, W. A. (1998) Unblocking of chain-terminated primer by HIV-1 reverse transcriptase through a nucleotide-dependent mechanism. *Proc. Natl. Acad. Sci. U.S.A.* **95,** 13471–13476
14. Tu, X., Das, K., Han, Q., Bauman, J. D., Clark, A. D., Jr., Hou, X., Frenkel, Y. V., Gaffney, B. L., Jones, R. A., Boyer, P. L., Hughes, S. H., Sarafianos, S. G., and Arnold, E. (2010) Structural basis of HIV-1 resistance to AZT by excision. *Nat. Struct. Mol. Biol.* **17,** 1202–1209
15. Arion, D., Kaushik, N., McCormick, S., Borkow, G., and Parniak, M. A. (1998) Phenotypic mechanism of HIV-1 resistance to 3′-azido-3′-deoxythymidine (AZT). Increased polymerization processivity and enhanced sensitivity to pyrophosphate of the mutant viral reverse transcriptase. *Biochemistry* **37,** 15908–15917
16. Lin, P. F., Samanta, H., Rose, R. E., Patick, A. K., Trimble, J., Bechtold, C. M., Revie, D. R., Khan, N. C., Federici, M. E., Li, H., *et al.* (1994) Genotypic and phenotypic analysis of human immunodeficiency virus type 1 isolates from patients on prolonged stavudine therapy. *J. Infect. Dis.* **170,** 1157–1164
17. Larder, B. A., and Kemp, S. D. (1989) Multiple mutations in HIV-1 reverse transcriptase confer high level resistance to zidovudine (AZT). *Science* **246,** 1155–1158
18. Nikolenko, G. N., Delviks-Frankenberry, K. A., Palmer, S., Maldarelli, F.,

Fivash, M. J., Jr., Coffin, J. M., and Pathak, V. K. (2007) Mutations in the connection domain of HIV-1 reverse transcriptase increase 3′-azido-3′-deoxythymidine resistance. *Proc. Natl. Acad. Sci. U.S.A.* **104,** 317–322

19. Yap, S. H., Sheen, C. W., Fahey, J., Zanin, M., Tyssen, D., Lima, V. D., Wynhoven, B., Kuiper, M., Sluis-Cremer, N., Harrigan, P. R., and Tachedjian, G. (2007) N348I in the connection domain of HIV-1 reverse transcriptase confers zidovudine and nevirapine resistance. *PLoS Med.* **4,** e335
20. Hachiya, A., Kodama, E. N., Sarafianos, S. G., Schuckmann, M. M., Sakagami, Y., Matsuoka, M., Takiguchi, M., Gatanaga, H., and Oka, S. (2008) Amino acid mutation N348I in the connection subdomain of human immunodeficiency virus type 1 reverse transcriptase confers multiclass resistance to nucleoside and non-nucleoside reverse transcriptase inhibitors. *J. Virol.* **82,** 3261–3270
21. Hachiya, A., Shimane, K., Sarafianos, S. G., Kodama, E. N., Sakagami, Y., Negishi, F., Koizumi, H., Gatanaga, H., Matsuoka, M., Takiguchi, M., and Oka, S. (2009) Clinical relevance of substitutions in the connection subdomain and RNase H domain of HIV-1 reverse transcriptase from a cohort of antiretroviral treatment-naive patients. *Antiviral Res.* **82,** 115–121
22. Paredes, R., Puertas, M. C., Bannister, W., Kisic, M., Cozzi-Lepri, A., Pou, C., Bellido, R., Betancor, G., Bogner, J., Gargalianos, P., Bánhegyi, D., Clotet, B., Lundgren, J., Menéndez-Arias, L., and Martinez-Picado, J., and EuroSIDA Study Group (2011) A376S in the connection subdomain of HIV-1 reverse transcriptase confers increased risk of virological failure to nevirapine therapy. *J. Infect. Dis.* **204,** 741–752
23. Gupta, S., Fransen, S., Paxinos, E. E., Stawiski, E., Huang, W., and Petropoulos, C. J. (2010) Combinations of mutations in the connection domain of human immunodeficiency virus type 1 reverse transcriptase. Assessing the impact on nucleoside and non-nucleoside reverse transcriptase inhibitor resistance. *Antimicrob. Agents Chemother.* **54,** 1973–1980
24. Delviks-Frankenberry, K. A., Nikolenko, G. N., Barr, R., and Pathak, V. K. (2007) Mutations in human immunodeficiency virus type 1 RNase H primer grip enhance 3′-azido-3′-deoxythymidine resistance. *J. Virol.* **81,** 6837–6845
25. Delviks-Frankenberry, K. A., Nikolenko, G. N., Boyer, P. L., Hughes, S. H., Coffin, J. M., Jere, A., and Pathak, V. K. (2008) HIV-1 reverse transcriptase connection subdomain mutations reduce template RNA degradation and enhance AZT excision. *Proc. Natl. Acad. Sci. U.S.A.* **105,** 10943–10948
26. Nikolenko, G. N., Delviks-Frankenberry, K. A., and Pathak, V. K. (2010) A novel molecular mechanism of dual resistance to nucleoside and non-nucleoside reverse transcriptase inhibitors. *J. Virol.* **84,** 5238–5249
27. Delviks-Frankenberry, K. A., Nikolenko, G. N., and Pathak, V. K. (2010) The "Connection" between HIV drug resistance and RNase H. *Viruses* **2,** 1476–1503
28. Biondi, M. J., Beilhartz, G. L., McCormick, S., and Götte, M. (2010) N348I in HIV-1 reverse transcriptase can counteract the nevirapine-mediated bias toward RNase H cleavage during plus-strand initiation. *J. Biol. Chem.* **285,** 26966–26975
29. Larder, B. A., Kemp, S. D., and Harrigan, P. R. (1995) Potential mechanism for sustained antiretroviral efficacy of AZT-3TC combination therapy. *Science* **269,** 696–699
30. Whitcomb, J. M., Parkin, N. T., Chappey, C., Hellmann, N. S., and Petropoulos, C. J. (2003) Broad nucleoside reverse-transcriptase inhibitor cross resistance in human immunodeficiency virus type 1 clinical isolates. *J. Infect. Dis.* **188,** 992–1000
31. Lanier, E. R., Givens, N., Stone, C., Griffin, P., Gibb, D., Walker, S., Tisdale, M., Irlbeck, D., Underwood, M., St Clair, M., and Ait-Khaled, M. (2004) Effect of concurrent zidovudine use on the resistance pathway selected by abacavir-containing regimens. *HIV Med.* **5,** 394–399
32. Larder, B. A. (1994) Interactions between drug resistance mutations in human immunodeficiency virus type 1 reverse transcriptase. *J. Gen. Virol.* **75,** 951–957
33. Parikh, U. M., Bacheler, L., Koontz, D., and Mellors, J. W. (2006) The K65R mutation in human immunodeficiency virus type 1 reverse transcriptase exhibits bidirectional phenotypic antagonism with thymidine analog mutations. *J. Virol.* **80,** 4971–4977
34. Parikh, U. M., Zelina, S., Sluis-Cremer, N., and Mellors, J. W. (2007) Molecular mechanisms of bidirectional antagonism between K65R and thymidine analog mutations in HIV-1 reverse transcriptase. *AIDS* **21,** 1405–1414
35. Selmi, B., Deval, J., Alvarez, K., Boretto, J., Sarfati, S., Guerreiro, C., and Canard, B. (2003) The Y181C substitution in 3′-azido-3′-deoxythymidine-resistant human immunodeficiency virus, type 1, reverse transcriptase suppresses the ATP-mediated repair of the 3′-azido-3′-deoxythymidine 5′-monophosphate-terminated primer. *J. Biol. Chem.* **278,** 40464–40472
36. Byrnes, V. W., Emini, E. A., Schleif, W. A., Condra, J. H., Schneider, C. L., Long, W. J., Wolfgang, J. A., Graham, D. J., Gotlib, L., Schlabach, A. J., *et al.* (1994) Susceptibilities of human immunodeficiency virus type 1 enzyme and viral variants expressing multiple resistance-engendering amino acid substitutions to reserve transcriptase inhibitors. *Antimicrob. Agents Chemother.* **38,** 1404–1407
37. Frankel, F. A., Marchand, B., Turner, D., Götte, M., and Wainberg, M. A. (2005) Impaired rescue of chain-terminated DNA synthesis associated with the L74V mutation in human immunodeficiency virus type 1 reverse transcriptase. *Antimicrob. Agents Chemother.* **49,** 2657–2664
38. Miranda, L. R., Götte, M., Liang, F., and Kuritzkes, D. R. (2005) The L74V mutation in human immunodeficiency virus type 1 reverse transcriptase counteracts enhanced excision of zidovudine monophosphate associated with thymidine analog resistance mutations. *Antimicrob. Agents Chemother.* **49,** 2648–2656
39. Menéndez-Arias, L. (2008) Mechanisms of resistance to nucleoside analog inhibitors of HIV-1 reverse transcriptase. *Virus Res.* **134,** 124–146
40. Svicher, V., Sing, T., Santoro, M. M., Forbici, F., Rodríguez-Barrios, F., Bertoli, A., Beerenwinkel, N., Bellocchi, M. C., Gago, F., d'Arminio Monforte, A., Antinori, A., Lengauer, T., Ceccherini-Silberstein, F., and Perno, C. F. (2006) Involvement of novel human immunodeficiency virus type 1 reverse transcriptase mutations in the regulation of resistance to nucleoside inhibitors. *J. Virol.* **80,** 7186–7198
41. Garriga, C., Pérez-Elías, M. J., Delgado, R., Ruiz, L., Pérez-Alvarez, L., Pumarola, T., López-Lirola, A., González-García, J., Menéndez-Arias, L., and Spanish Group for the Study of Antiretroviral Drug Resistance (2009) HIV-1 reverse transcriptase thumb subdomain polymorphisms associated with virological failure to nucleoside drug combinations. *J. Antimicrob. Chemother.* **64,** 251–258
42. Hachiya, A., Aizawa-Matsuoka, S., Tanaka, M., Takahashi, Y., Ida, S., Gatanaga, H., Hirabayashi, Y., Kojima, A., Tatsumi, M., and Oka, S. (2001) Rapid and simple phenotypic assay for drug susceptibility of human immunodeficiency virus type 1 using CCR5-expressing HeLa/CD4(+) cell clone 1–10 (MAGIC-5). *Antimicrob. Agents Chemother.* **45,** 495–501
43. Hachiya, A., Gatanaga, H., Kodama, E., Ikeuchi, M., Matsuoka, M., Harada, S., Mitsuya, H., Kimura, S., and Oka, S. (2004) Novel patterns of nevirapine resistance-associated mutations of human immunodeficiency virus type 1 in treatment-naive patients. *Virology* **327,** 215–224
44. Hachiya, A., Kodama, E. N., Schuckmann, M. M., Kirby, K. A., Michailidis, E., Sakagami, Y., Oka, S., Singh, K., and Sarafianos, S. G. (2011) K70Q adds high level tenofovir resistance to "Q151M complex" HIV reverse transcriptase through the enhanced discrimination mechanism. *PLoS One* **6,** e16242
45. Schuckmann, M. M., Marchand, B., Hachiya, A., Kodama, E. N., Kirby, K. A., Singh, K., and Sarafianos, S. G. (2010) The N348I mutation at the connection subdomain of HIV-1 reverse transcriptase decreases binding to nevirapine. *J. Biol. Chem.* **285,** 38700–38709
46. Michailidis, E., Marchand, B., Kodama, E. N., Singh, K., Matsuoka, M., Kirby, K. A., Ryan, E. M., Sawani, A. M., Nagy, E., Ashida, N., Mitsuya, H., Parniak, M. A., and Sarafianos, S. G. (2009) Mechanism of inhibition of HIV-1 reverse transcriptase by 4′-ethynyl-2-fluoro-2′-deoxyadenosine triphosphate, a translocation-defective reverse transcriptase inhibitor. *J. Biol. Chem.* **284,** 35681–35691
47. Marchand, B., and Götte, M. (2003) Site-specific footprinting reveals differences in the translocation status of HIV-1 reverse transcriptase. Implications for polymerase translocation and drug resistance. *J. Biol. Chem.* **278,** 35362–35372
48. Bauman, J. D., Das, K., Ho, W. C., Baweja, M., Himmel, D. M., Clark, A. D., Jr., Oren, D. A., Boyer, P. L., Hughes, S. H., Shatkin, A. J., and Arnold, E. (2008) Crystal engineering of HIV-1 reverse transcriptase for structure-based drug design. *Nucleic Acids Res.* **36,** 5083–5092

49. Leslie, A. G. W., and Powell, H. R. (2007) in *Evolving Methods for Macromolecular Crystallography* (Read, R. J., and Sussman, J. L., eds) pp. 41–51, Springer, Dordrecht, The Netherlands
50. McCoy, A. J., Grosse-Kunstleve, R. W., Adams, P. D., Winn, M. D., Storoni, L. C., and Read, R. J. (2007) Phaser crystallographic software. *J. Appl. Crystallogr.* **40,** 658–674
51. Emsley, P., Lohkamp, B., Scott, W. G., and Cowtan, K. (2010) Features and development of Coot. *Acta Crystallogr. D Biol. Crystallogr.* **66,** 486–501
52. Brünger, A. T., Adams, P. D., Clore, G. M., DeLano, W. L., Gros, P., Grosse-Kunstleve, R. W., Jiang, J. S., Kuszewski, J., Nilges, M., Pannu, N. S., Read, R. J., Rice, L. M., Simonson, T., and Warren, G. L. (1998) Crystallography and NMR system. A new software suite for macromolecular structure determination. *Acta Crystallogr. D Biol. Crystallogr.* **54,** 905–921
53. Murshudov, G. N., Vagin, A. A., and Dodson, E. J. (1997) Refinement of macromolecular structures by the maximum-likelihood method. *Acta Crystallogr. D Biol. Crystallogr.* **53,** 240–255
54. Boyer, P. L., Sarafianos, S. G., Arnold, E., and Hughes, S. H. (2002) Nucleoside analog resistance caused by insertions in the fingers of human immunodeficiency virus type 1 reverse transcriptase involves ATP-mediated excision. *J. Virol.* **76,** 9143–9151
55. Sarafianos, S. G., Das, K., Hughes, S. H., and Arnold, E. (2004) Taking aim at a moving target. Designing drugs to inhibit drug-resistant HIV-1 reverse transcriptases. *Curr. Opin. Struct. Biol.* **14,** 716–730
56. Das, K., Sarafianos, S. G., Clark, A. D., Jr., Boyer, P. L., Hughes, S. H., and Arnold, E. (2007) Crystal structures of clinically relevant K103N/Y181C double mutant HIV-1 reverse transcriptase in complexes with ATP and non-nucleoside inhibitor HBY 097. *J. Mol. Biol.* **365,** 77–89
57. Sarafianos, S. G., Clark, A. D., Jr., Das, K., Tuske, S., Birktoft, J. J., Ilankumaran, P., Ramesha, A. R., Sayer, J. M., Jerina, D. M., Boyer, P. L., Hughes, S. H., and Arnold, E. (2002) Structures of HIV-1 reverse transcriptase with pre- and post-translocation AZTMP-terminated DNA. *EMBO J.* **21,** 6614–6624
58. Clark, S. A., Shulman, N. S., Bosch, R. J., and Mellors, J. W. (2006) Reverse transcriptase mutations 118I, 208Y, and 215Y cause HIV-1 hypersusceptibility to non-nucleoside reverse transcriptase inhibitors. *AIDS* **20,** 981–984
59. Zelina, S., Sheen, C. W., Radzio, J., Mellors, J. W., and Sluis-Cremer, N. (2008) Mechanisms by which the G333D mutation in human immunodeficiency virus type 1 Reverse transcriptase facilitates dual resistance to zidovudine and lamivudine. *Antimicrob. Agents Chemother.* **52,** 157–163
60. Ehteshami, M., Beilhartz, G. L., Scarth, B. J., Tchesnokov, E. P., McCormick, S., Wynhoven, B., Harrigan, P. R., and Götte, M. (2008) Connection domain mutations N348I and A360V in HIV-1 reverse transcriptase enhance resistance to 3′-azido-3′-deoxythymidine through both RNase H-dependent and -independent mechanisms. *J. Biol. Chem.* **283,** 22222–22232
61. Radzio, J., Yap, S. H., Tachedjian, G., and Sluis-Cremer, N. (2010) N348I in reverse transcriptase provides a genetic pathway for HIV-1 to select thymidine analog mutations and mutations antagonistic to thymidine analog mutations. *AIDS* **24,** 659–667
62. Geleziunas, R., Gallagher, K., Zhang, H., Bacheler, L., Garber, S., Wu, J. T., Shi, G., Otto, M. J., Schinazi, R. F., and Erickson-Viitanen, S. (2003) HIV-1 resistance profile of the novel nucleoside reverse transcriptase inhibitor β-D-2′,3′-dideoxy-2′,3′-didehydro-5-fluorocytidine (Reverset). *Antivir. Chem. Chemother.* **14,** 49–59
63. Hanson, K., and Hicks, C. (2006) New antiretroviral drugs. *Curr. HIV/AIDS Rep.* **3,** 93–101
64. Hammond, J. L., Parikh, U. M., Koontz, D. L., Schlueter-Wirtz, S., Chu, C. K., Bazmi, H. Z., Schinazi, R. F., and Mellors, J. W. (2005) *In vitro* selection and analysis of human immunodeficiency virus type 1 resistant to derivatives of β-2′,3′-didehydro-2′,3′-dideoxy-5-fluorocytidine. *Antimicrob. Agents Chemother.* **49,** 3930–3932

Cell. Mol. Biol. 58 (1): 187-195
Published on December 22, 2012
DOI 10.1170/T940

Cellular & Molecular Biology
http://www.cellmolbiol.com
Copyright © 2012. All rights reserved.

EFFECT OF TRANSLOCATION DEFECTIVE REVERSE TRANSCRIPTASE INHIBITORS ON THE ACTIVITY OF N348I, A CONNECTION SUBDOMAIN DRUG RESISTANT HIV-1 REVERSE TRANSCRIPTASE MUTANT

E. MICHAILIDIS[1], K. SINGH[1], E. M. RYAN[1], A. HACHIYA[1], Y. T. ONG[1], K. A. KIRBY[1], B. MARCHAND[1], E. N. KODAMA[2], H. MITSUYA[3], M. A. PARNIAK[4] AND S. G. SARAFIANOS[1,5]✉

[1] Christopher S. Bond Life Sciences Center, Department of Molecular Microbiology & Immunology, Columbia, MO 65211, USA
[2] Division of Emerging Infectious Diseases, Tohoku University School of Medicine, Sendai 980-8575, Japan
[3] Department of Hematology and Infectious Diseases, Kumamoto University, Kumamoto 860-8556, Japan & Experimental Retrovirology Section, HIV/AIDS Malignancy Branch, NIH, Bethesda, MD 20892, USA
[4] Department of Molecular Genetics & Biochemistry University of Pittsburgh School of Medicine, Pittsburgh, PA 15261, USA
[5] Department of Biochemistry, University of Missouri, Columbia, MO 65211, USA

Abstract

4'-Ethynyl-2-fluoro-2'-deoxyadenosine (EFdA) is a highly potent inhibitor of HIV-1 reverse transcriptase (RT). We have previously shown that its exceptional antiviral activity stems from a unique mechanism of action that is based primarily on blocking translocation of RT; therefore we named EFdA a Translocation Defective RT Inhibitor (TDRTI). The N348I mutation at the connection subdomain (CS) of HIV-1 RT confers clinically significant resistance to both nucleoside (NRTIs) and non-nucleoside RT inhibitors (NNRTIs). In this study we tested EFdA-triphosphate (TP) together with a related compound, ENdA-TP (4'-ethynyl-2-amino-2'-deoxyadenosine triphosphate) against HIV-1 RTs that carry clinically relevant drug resistance mutations: N348I,D67N/K70R/L210Q/T215F, D67N/K70R/L210Q/T215F/N348I, and A62V/V75I/F77L/F116Y/Q151M. We demonstrate that these enzymes remain susceptible to TDRTIs. Similar to WT RT, the N348I RT is inhibited by EFdA mainly at the point of incorporation through decreased translocation. In addition, the N348I substitution decreases the RNase H cleavage of DNA terminated with EFdA-MP ($T/P_{EFdA-MP}$). Moreover, N348I RT unblocks EFdA-terminated primers with similar efficiency as the WT enzyme, and further enhances EFdA unblocking in the background of AZT-resistance mutations. This study provides biochemical insights into the mechanism of inhibition of N348I RT by TDRTIs and highlights the excellent efficacy of this class of inhibitors against WT and drug-resistant HIV-1 RTs.

Key words: EFdA, ENdA, N348I, Translocation Defective Reverse Transcriptase Inhibitors, Reverse Transcriptase, HIV-1, Antivirals.

Article information

Received on June 15, 2012
Accepted on September 2, 2012

✉ **Corresponding author**
Tel: +1 (573) 882-4338
Fax: +1 (573) 884 - 9676
E-mail:sarafianoss@missouri.edu

INTRODUCTION

Human immunodeficiency type 1 reverse transcriptase (HIV-1 RT) is a key enzyme that converts single-stranded genomic RNA into double-stranded DNA, which in turn is transported to the nucleus and integrated into the host cellgenome. The HIV-1 RT catalyzes both the RNA-and DNA-dependent DNA polymerase, and RNase H activities (11).The functional form of HIV-1 RT is a heterodimer consisting of p66 and p51 polypeptides (16). The p66 subunit has both enzymatic activities and includes the polymerase and the RNase H domains. The polymerase domain consists of the fingers, palm and thumb subdomains which are analogous to a right hand connected to the RNase H domain through the connection subdomain (42) (Fig. 1).

The p51 subunit lacks the RNase H domain and has been proposed to play a structural role (42), although recent work from our laboratory has also shown that mutations in the p51 subunit affect the polymerase and RNase H enzymatic functions of RT (38).

Highly active antiretroviral therapies (HAART) have been very effective in suppressing viral loads and having a significant impact on the life expectancy of HIV patients. Key components of HAART are drugs that target HIV RT. The two classes of RT inhibitors currently used in the clinic are nucleoside-nucleotide RT inhibitors (NRTI) and non-nucleoside RT inhibitors (NNRTI). NRTIs inhibit RT by acting as chain-terminators after they are incorporated into the nascent DNA chain. NNRTIs act noncompetitively by binding to a hydrophobic pocket adjacent to, but distinct from the polymerase active site of RT and by imposing rigidity to the movements of thumb subdomain required for efficient polymerase function (20, 22, 35, 37, 39, 41).

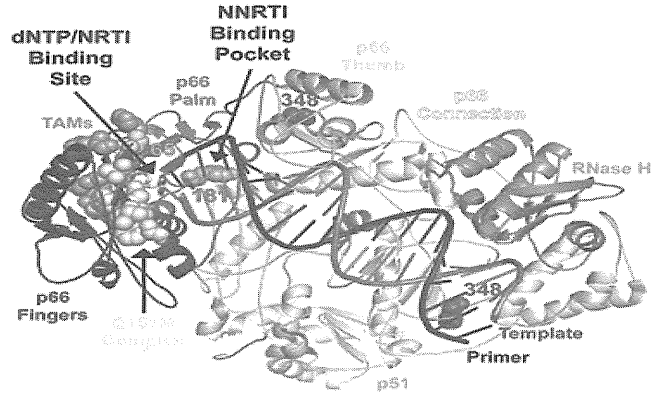

Figure 1. HIV-1 RT structure with highlighted residues of drug-resistance. The RT color scheme is as follows: fingers in blue, palm in red, thumb in green, connection in yellow, RNase H in orange, and p51 in gray. The Q151M complex is shown in cyan, TAMs in magenta, and 348 residue in purple. The RT coordinates are from PDB ID 1T05. The figure was made using PyMOL.

Despite the phenomenal success of HAART regimens, continuous use of antivirals leads to the emergence of viruses that are resistant to all known anti-AIDS drugs. The mutations associated with NNRTI resistanceare generally located at the NNRTI binding pocket (NNIBP). However, the mutations that cause resistance to NRTIs have been noted to be scattered in the polymerase domain (22, 39). While most NNRTI and NRTI resistance mutations are at the palm and fingers subdomains of HIV-1 RT, it has recently been shown that some mutations associated with NNRTI and NRTI resistance are at the connection and RNase H regions of RT (6, 8, 13, 15, 17, 29, 43). The most significant of these mutations is N348I, which confers moderate resistance to both NRTIs and NNRTIs, and is present in a significant number of clinical isolates, especially in the presence of other NRTI mutations.

In light of the new emerging drug resistance mutations, it is essential to identify inhibitors that are very potent and effective against viral strains that are resistant to all approved therapeutics. One such inhibitor is 4'-ethynyl-2-fluoro-2'-deoxyadenosine triphosphate (EFdA-TP) (18, 19). We have recently reported the mechanism of HIV inhibition by EFdA (26).In contrast to other approved NRTIs, which have a modification at 3'OH, EFdA contains a 3'OH moiety and blocks DNA synthesis by locking the primer terminus at the pre-translocation site of HIV-1 RT. In addition to EFdA, we have recently shown that ENdA also inhibits HIV RT potently acting as a TDRTI (data not shown).

Recently, using transient-state kinetic experiments we established the mechanism of NNRTI resistance of HIV-1 RT containing the N348I mutation at the connection subdomain of the enzyme (38).We showed that the resistance to the NNRTI nevirapine (NEV) is primarily the result of changes distant from the NNRTI binding pocket, which decrease inhibitor binding (increase $K_{d\text{-}NVP}$) by primarily decreasing the association rate of the inhibitor ($k_{on\text{-}NVP}$). Moreover, the N348I mutation increased nucleic acid binding affinity, enhanced processivity and lowered the catalytic turnover rate of the natural substrate. In this study we determine the ability of TDRTIs to block reverse transcription by the multi-drug resistant N348I HIV-1 RT as well as other NRTI resistant RTs, D67N/K70R/L210Q/T215F (resistant to AZT by the excision mechanism) D67N/K70R/L210Q/T215F/N348I, and A62V/V75I/F77L/F116Y/Q151M (multidrug resistant to AZT and dideoxynucleotide RT inhibitors).

MATERIALS AND METHODS

Enzymes and Nucleic acids

The RT genes coding for p66 and p51 subunits of BH10 HIV-1 were cloned in the pETDuet-1 vector (Novagen) using restriction sites *NcoI* and *SacI* for the p51 subunit, and *SacII* and *AvrII* for the p66 subunit (2, 38). The sequences coding for a hexa-histidine tag and the 3C protease recognition sequence were added at the N terminus of the p51 subunit. RT was expressed in BL21 (Invitrogen) and purified by nickel affinity chromatography and monoQ anion exchange chromatography (33). Oligonucleotides used in this study were chemically synthesized and purchased from Integrated DNA Technologies (Coralville, IA). Sequences of the DNA substrates are shown in Table 1. Deoxynucleotide triphosphates and dideoxynucleotide triphosphates were purchased from Fermentas (Glen Burnie, MD). EFdA and ENdA were synthesized by Yamasa Corporation (Chiba, Japan) as described before (30). Using EFdA and ENdA as starting material the triphosphate forms EFdA-TP and ENdA-TP were synthesized by Tri-Link BioTechnologies (San Diego, CA). Concentrations of nucleotides, EFdA-TP and ENdA-TP were calculated spectrophotometrically on the basis of absorption at 260 nm and their extinction coefficients. All nucleotides were treated with inorganic pyrophosphatase (Roche Diagnostics) as described previously (24) to remove traces of PPi contamination that might interfere with the rescue assay.

Primer extension assays

Inhibition of HIV-1 RT by TDRTIs

DNA template (T_{d31}) was annealed to 5'-Cy3 labeled DNA primer (P_{d18}). To monitor primer extension, the T_{d31}/5'Cy3-P_{d18} hybrid (20 nM) was incubated at 37°C with WT or drug-resistant HIV-1 RTs (20 nM) in a buffer containing 50 mM Tris (pH 7.8) and 50 mM NaCl (RT buffer). Varying amounts of EFdA-TP or ENdA-TP were added and the reactions were initiated by the addition of 6 mM $MgCl_2$to a final volume of 20 µl. All dNTPs were present at a final concentration of 1 µM. The reactions were terminated after 15 minutes by adding equal volume of 100% formamide containing traces of bromophenol blue. The products were resolved on a 15% polyacrylamide 7 M urea gel. In this and in subsequent assays, the gels were scanned with a PhosphorImager (FujiFilm FLA 5000), the bands for fully extended product were quantified using Multi Gauge (FujiFilm) and results were plotted using one

Table 1.DNA and RNA sequences used in this study.

Polymerization experiments	
T_{d31}	5'-CCA TAG ATA GCA TTG GTG CTC GAA CAG TGA C
T_{r31}	5'-CCA UAG AUA GCA UUG GUG CUC GAA CAG UGA C
P_{d18}	5'-Cy3-GTC ACT GTT CGA GCA CCA
Footprinting experiments	
T_{d43}	5'-Cy3-CCA TAG ATA GCA TTG GTG CTC GAA CAG TGA CAA TCA GTG TAGA
P_{d30}	5'-TCT ACA CTG ATT GTC ACT GTT CGA GCA CCA
RNase H experiments	
T_{r35}	5'-Cy3-GGA AAU CUC UAG CAG UGG CGC CCG AAC AGG GAC CU
P_{d25}	5'-AGG TCC CTG TTC GGG CGC CAC TGC T

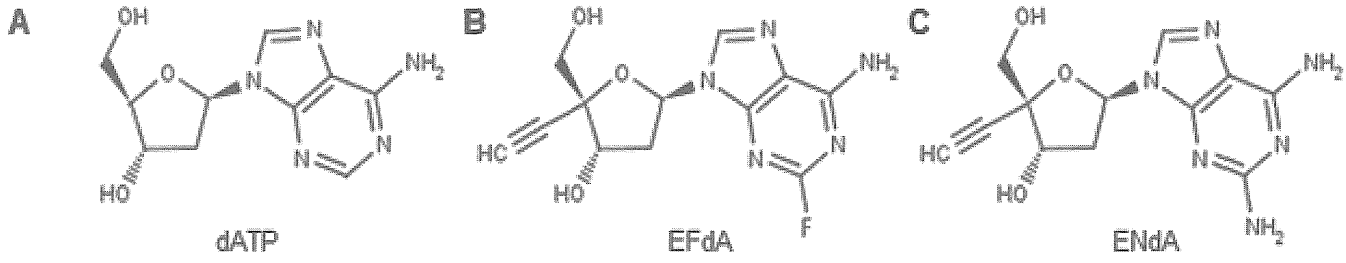

Figure 2. Chemical structures of dATP, EFdA and ENdA.

site competition equation on GraphPad Prism 4 to determine the IC_{50} for EFdA-TP and ENdA-TP.

Site-specific Fe^{2+} Footprinting Assay

Site-specific Fe^{2+} footprints were monitored on 5'-Cy3-labeled DNA templates. 100 nM of 5'Cy3-T_{d43}/P_{d20} was incubated with 600 nMWT or N348I RT in a buffer containing 120 mM sodium cacodylate (pH 7), 20 mM NaCl, 6 mM $MgCl_2$, and either of 5 μM ddATP or 1 μM EFdA-TP, to allow quantitative chain-termination. Prior to the treatment with Fe^{2+}, complexes were pre-incubated for 7 min with increasing concentrations of the next incoming nucleotide (dTTP). The complexes were treated with ammonium iron sulfate (1 mM) as previously described (21). This reaction relies on autoxidation of Fe^{2+}(3) to create a local concentration of hydroxyl radical which cleaves the DNA at the nucleotide closest to the Fe^{2+} specifically bound to the RNase H active site.

ATP-dependent Excision and Rescue assay

20 nM of purified $T_{d31}/P_{d18\text{-}EFdA\text{-}MP}$ or $T_{r31}/P_{d18\text{-}EFdA\text{-}MP}$ were incubated with 60 nM WT, N348I, D67N/K70R/L210Q/T215F or D67N/K70R/L210Q/T215F/N348I RT in the presence of 3.5 mM ATP, 100 M dATP, 0.5 μM dTTP, and 10 μM ddGTP in RT buffer and 10 mM $MgCl_2$. Aliquots of the reaction were stopped at different time points (0-90 min) and analyzed as described above.

RNase H Assays

RNase H assays were performed by incubating the RNA/DNA duplex 5'Cy3-T_{r35}/P_{d25} or 5'Cy3-$T_{r35}/P_{d25\text{-}ddAMP}$ or 5'Cy3-$T_{r35}/P_{d25\text{-}EFdA\text{-}MP}$ (50 nM) with WT or N348I RT (50 nM) in RT buffer at 37 °C with $MgCl_2$ (6 mM). Reactions were quenched after incubation (1–5 min) with equal volumes of formamide containing trace amounts of bromophenol blue. Reaction products were analyzed as before. The primary RNase H cleavage product is mainly 18 nucleotides from the 3'-end of the DNA primer (18 nucleotides), and the secondary cleavage product is mainly 12 nucleotides from the 3'-end of the primer (12 nucleotides) as reported previously (10, 12, 38).

RESULTS

The inhibitors used here to characterize the susceptibility of N348I to various drugs are adenosine analogs. The structures of these analogs are shown in Fig. 2. The normal deoxynucleotide dATP is shown in Fig. 2A. EFdA and ENdA are shown in Figs. 2B and 2C, respectively.It can be seen in these figures that unlike other anti-HIV NRTIs both EFdA and ENdA have a 3'OH. These compounds also contain an ethynyl group at the 4' position. EFdA and ENdA differ in their substitutions at the 2 position of the purine ring. EFdA at this position has fluorine whereas ENdA has an amino group.

Inhibition of WT and N348I mutant of HIV-1 RT

The inhibition of WT, N348I, D67N/K70R/L210Q/T215F, D67N/K70R/L210Q/T215F/N348I mutants of HIV-1 RT by EFdA-TP and ENdA-TP was assessed by a primer extension assay. As shown in Fig. 3A-3D, EFdA-TP and ENdA-TP suppressed RT-catalyzed DNA synthesis in a dose-dependent manner. The IC_{50}values for both analogs are shown in Table 2. N348I, D67N/K70R/L210Q/T215F and D67N/K70R/L210Q/T215F/N348I RTs were inhibited by EFdA-TP and ENdA-TP with similar efficiency compared to the WT enzyme. In addition, another mutant HIV-1 RT (A62V/V75I/F77L/F116Y/Q151M) was included in drug susceptibility assays (Fig. 3E-3G).

We have previously shown that EFdA inhibits DNA synthesis at the point of incorporation. Thus, we examined here the stopping patterns after incorporation products of the primer extension assay for the stopping patterns (Fig. 3). The primer synthesis shown in Fig. 3 clearly demonstrates that the stopping pattern follows the incorporation of adenosine analogs. Three distinct bands at positions 1, 6 and 10 indicate that both analogs inhibit RT mainly at the point of incorporation. Therefore, these compounds act primarily as obligate chain terminators. There is also an additional band at position 7, suggesting that in some

Table 2. IC_{50} values of EFdA-TP and ENdA-TP against WT and drug-resistant HIV-1 RTs.

Inhibitor/Enzyme	WT	N348I	D67N/K70R/ L210Q/T215F	D67N/K70R/L210Q/ T215F/N348I	A62V/V75I/F77L/ F116Y/Q151M
EFdA-TP (nM)	130	122	157	217	121
ENdA-TP (nM)	71	54	98	110	85

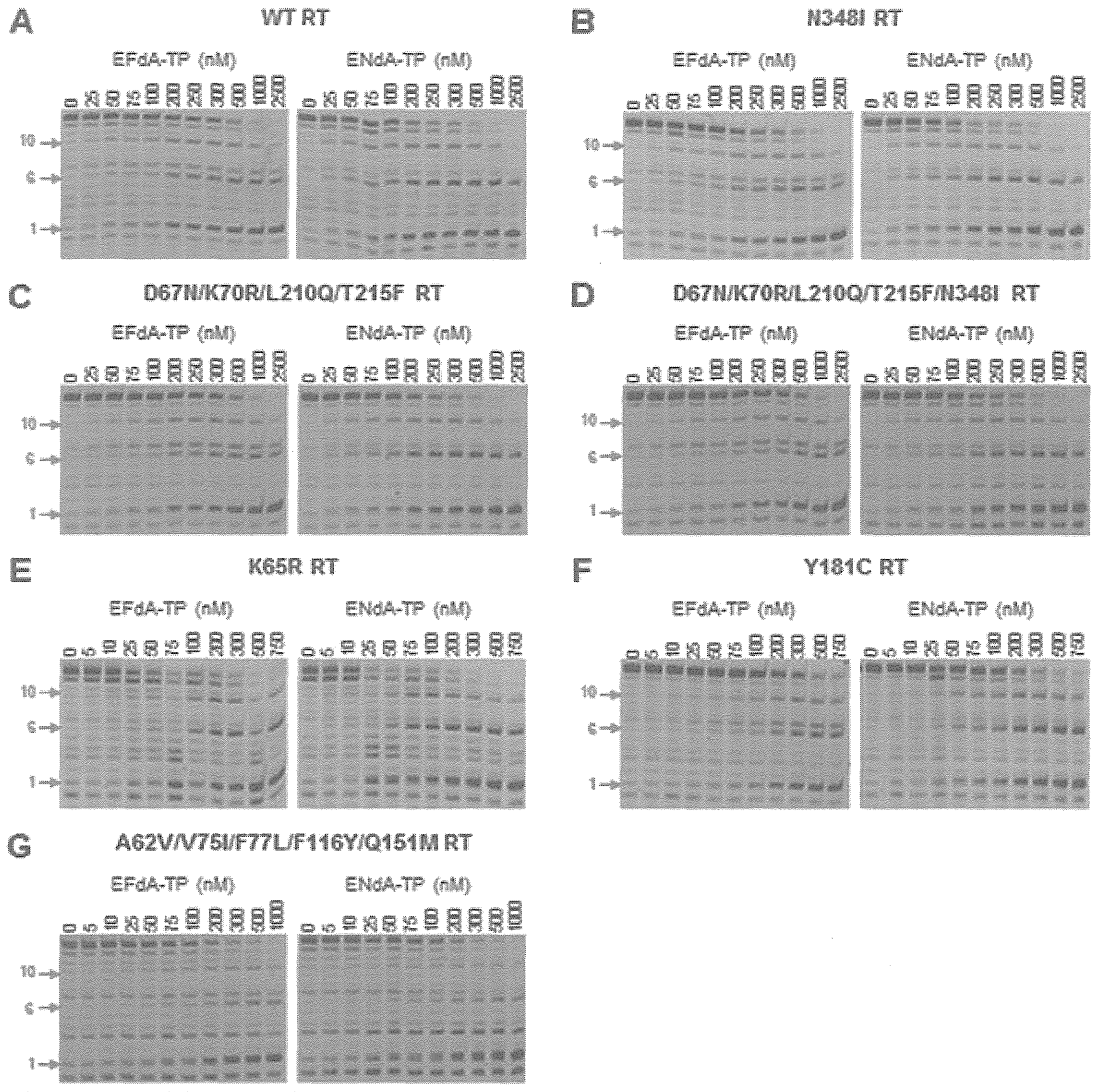

Figure 3. EFdA-TP and ENdA-TP inhibit WT and drug-resistant HIV-1 RTs. (A) T_{d31}/P_{d18} was incubated with various HIV-1 RTs for 15 minutes in the presence of 1μM dNTPs, $MgCl_2$ and increasing concentrations of EFdA-TP or ENdA-TP. The products synthesized by HIV-1 RT were quantified and plotted against increasing concentrations of the inhibitors. The IC_{50} values of the nucleotide analogs were determined by quantifying the percent of full extension and fitting the data points to GraphPad Prism 4 using one-site competition nonlinear regression (shown in Table 2). Arrows indicate the positions where dATP or dATP analogs are expected to be incorporated.

instances EFdA may allow addition of one nucleotide after its incorporation, thus acting as a delayed chain terminator (Fig. 3). This type of inhibition is far less common and is sequence-dependent. These finding agrees with our previous studies on WT RT (26).

Effect of EFdA-MP on Translocation of WT and N348I mutant of HIV-1 RT

The connection subdomain mutation N348I has been related to the altered DNA binding affinity and processivity of the mutant enzyme compared to the WT RT (4, 38). Since EFdA is a TDRTI and its incorporation is assumed to affect the translocation and thereby DNA binding and processivity, we investigated the translocation of EFdA-containing template-primers using the hydroxyl radical site-specific footprinting assay (21). The results of the footprinting assay shown in Fig. 4 demonstrate that the presence of EFdA-MP at the 3'end of the DNA primer blocks translocation and prevents incorporation of the next incoming dNTP. Therefore, similar to WT RT, the mutant N348I RT is also inhibited by EFdA-TP *via* the same mechanism.

Effect of EFdA-MP on RNase H activity of WT and N348I RTs

The template/primers containing EFdA-MP, ddAMP, or without inhibitor incorporated at the 3'end of the primer were used in RNase H assays with WT and N348I RTs in a time dependent manner. As previously noted, Fig. 5 shows that N348I mutant RT has decreased RNase H activity for all substrates used in this assay. The RNase H assays carried out in presence of T/P trap showed the disappearance of the secondary cuts for both enzymes used here. This is likely due to a defect in translocation that EFdA imposes on the enzyme. Interestingly, the primary cut of EFdA-teminated primers is a single band when the T/P has EFdA, but not ddA at the 3' primer terminus. Moreover, the RNA cleavage of $T_{r35}/P_{d25\text{-}EFdA\text{-}MP}$ was less than that of $T_{r35}/P_{d25\text{-}ddAMP}$ or T_{r35}/P_{d25} possibly because of less favorable positioning at the RNase H of T/P with EFdA at the 3' terminus.

ATP-dependent unblocking of EFdA-MP terminated primers by WT and N348I RTs

Since EFdA-MP-terminated primers bind predominantly in a pre-translocation mode we expected that EFdA-MP will be efficiently unblocked by both WT and N348I RTs.

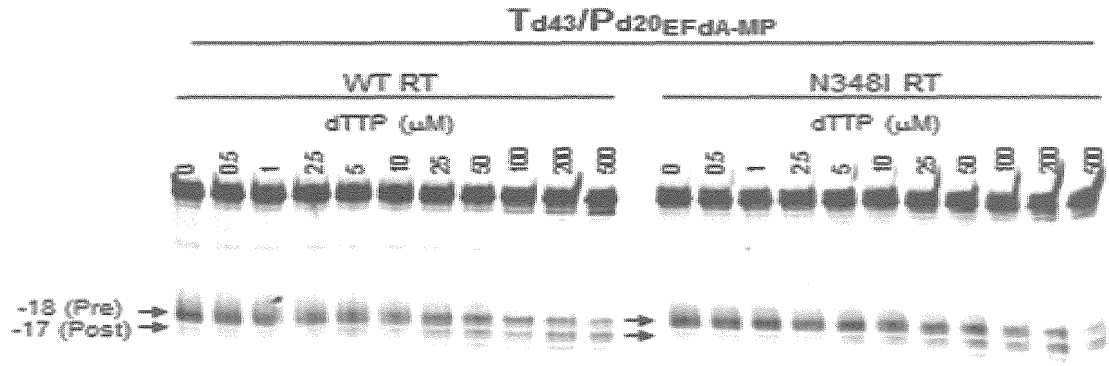

Figure 4. Determination of the translocation state of WT or N348I HIV-1 RT bound to $T_{d43}/P_{20\text{-}EFdA\text{-}MP}$. The translocation state of RT after EFdA-MP incorporation was determined using site-specific Fe^{2+}footprinting. $T_{d43}/P_{d30\text{-}EFdA\text{-}MP}$ (100 nM) with 5'-Cy3 label on the DNA template was incubated with HIV-1 RT (600 nM) and various concentrations of the next incoming nucleotide (dTTP). The complexes were treated for 5 min with ammonium iron sulfate (1 mM) and resolved on a polyacrylamide 7 M urea gel. An excision at position 18 indicates a pre-translocation complex, whereas the excision at position 17 represents a post-translocation complex. In both WT and N348I RT EFdA-MP prevents translocation with similar efficiency.

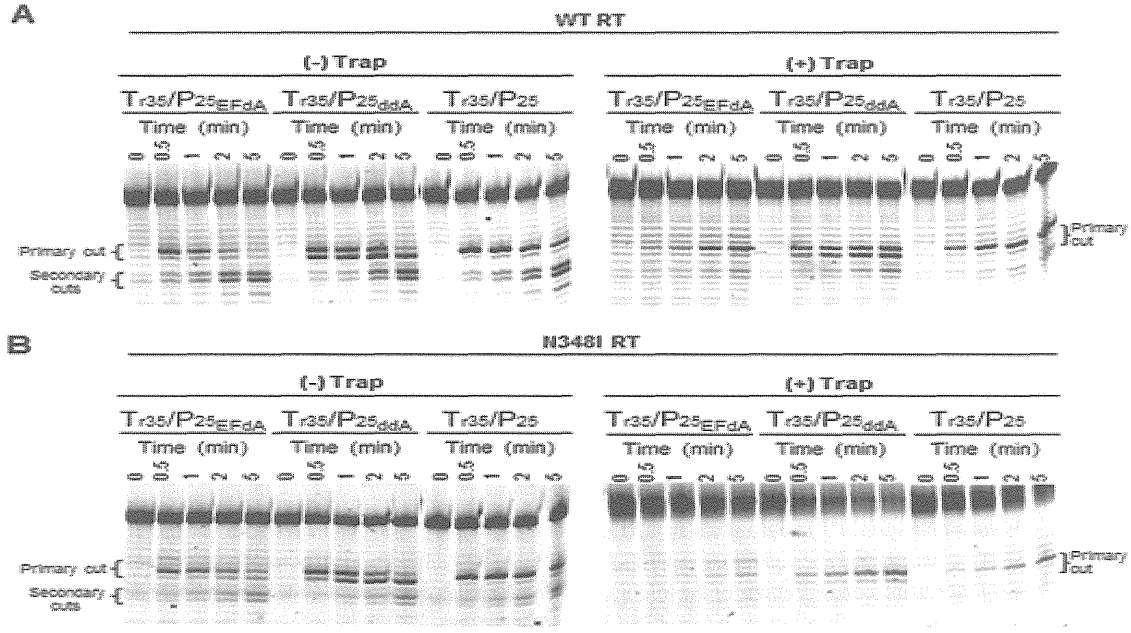

Figure 5. Effect of EFdA on RNase H activity of WT and N348I HIV-1 RTs. 50 nM Cy3-$T_{r35}/P_{d25\text{-}EFdA\text{-}MP}$ or Cy3-$T_{r35}/P_{d25\text{-}ddAMP}$ or Cy3-T_{r35}/P_{d25} was incubated with 50 nMWT (A) or N348I (B) HIV-1 RT for varying times (0-5 minutes) at 37°C in RT buffer. The experiment was carried out in the presence or absence of non-labeled T_{d35}/P_{d25} trap (25 μM). Reactions were initiated with the addition of $MgCl_2$ and stopped with formamide. The primary and secondary cuts are indicated in the gel images.

The ATP-dependent excision and subsequent rescue of EFdA-MP primers is shown in Fig. 6. The bands marked as 'Rescued Primer" have comparable product for the WT and N348I mutant enzyme for both DNA (Fig. 6A) and RNA (Fig. 6B) templates suggesting that resistance mutant N348I does not have any significant effect on the unblocking of EFdA-MP containing primers (RNA *vs.* DNA) (Fig. 6). However, the N348I mutation in the background of AZT resistance mutations D67N, K70R, L210Q and T215F showed a 2-fold increase in unblocking EFdA-MP containing primers both with DNA and RNA templates (Fig. 6).

DISCUSSION

There are currently more than 20 antiretrovirals that have been approved by the US Food and Drug Administration for the treatment of HIV infection. They fall into four categories, targeting HIV RT, protease, integrase, the entry step, and the fusion of the viral and cell membranes. RT inhibitors are either NRTIs or NNRTIs.The NRTIs-such zidovudine (AZT) and lamivudine compete with the natural substrates and get incorporated into the nascent DNA chain, blocking further polymerization because they lack a 3'OH group required for DNA synthesis. NNRTIs such as nevirapine and efavirenz inhibit the polymerase activity of RT by binding at a hydrophobic pocket nearly 10 Å away from the polymerase active site (Fig. 1). This pocket is created after the binding of NNRTIs. The highly active antiretroviral therapy (HAART) introduced in the mid-90s contains the combination of antivirals (generally a protease inhibitor and two NRTIs or an NNRTI and two NRTIs) targets the replication of the resistant virus.

Extended or incomplete treatments with antiretrovirals result in the emergence of drug resistance mutations. In the case of drugs that target RT, most of the resistance mutations were found to be present in the polymerase domain of RT. These resistance mutations against NRTIs function primarily with two mechanisms: (i) they reduce the binding affinity/incorporation of NRTI (34, 40) or (ii) enhance

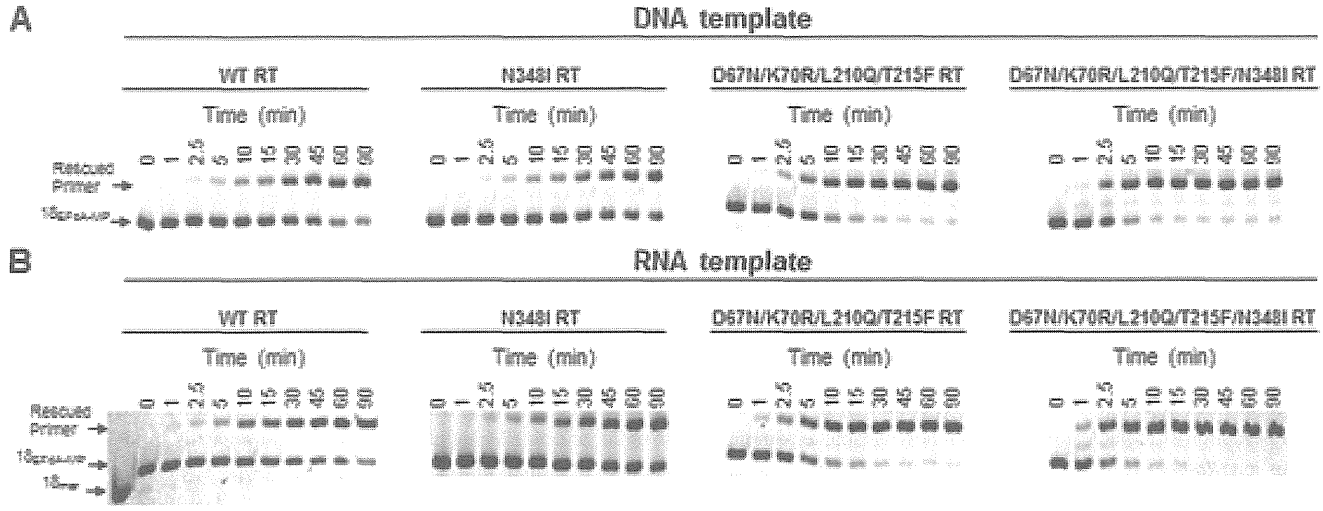

C

Rates of ATP-mediated rescue (min^{-1})

	WT RT	N348I RT	D67N/K70R/L210Q/T215F RT	D67N/K70R/L210Q/T215F/N348I RT
DNA template	0.030 (1)	0.028 (0.9)	0.112 (3.7)	0.240 (8)
RNA template	0.037 (1)	0.025 (0.7)	0.154 (4.2)	0.369 (10)

Figure 6. ATP-dependent unblocking of EFdA-MP terminated primers. ATP-dependent rescue of $T_{d31}/P_{d18\text{-}EFdA\text{-}MP}$ (A) and $T_{r31}/P_{d18\text{-}EFdA\text{-}MP}$ (B). Purified $T/P_{EFdA\text{-}MP}$ was incubated with WT, N348I, D67N/K70R/L210Q/T215F or D67N/K70R/L210Q/T215F/N348I HIV-1 RT in the presence of ATP (3.5 mM), dATP (100 μM), dTTP (0.5 μM), ddGTP (10 μM) and 10 mM $MgCl_2$ at 37 °C. Aliquots of the reaction were stopped at the indicated time points (0-90 min). (C) The rates of the ATP-dependent rescue of EFdA-MP terminated primers were calculated after quantifying the rescued products and plotting to the burst equation in GraphPad Prism 4.

the selective excision of incorporated NRTI from a chain-terminated primer terminus (9, 23-25, 36). The resistance against NNRTIs is primarily through the mutations that reduce the binding affinity of NNRTIs (7, 31, 32,35).

Recent studies showed that connection subdomain mutations can confer resistance to NRTIs. Nikolenko et al. suggested that some of these mutations increase AZT resistance by reducing template RNA degradation, thereby preserving the RNA template and providing additional time for RT to excise AZT monophosphate (27, 28). Hachiya et al., (13) as well as another research group (43) identified a clinical isolatewith phenotypic resistance to nevirapine (NVP) in the absence of known NNRTI mutations. This resistance was shown to be caused by N348I, a mutation at the connection subdomain of HIV-1RT. This mutation is not a polymorphism, as it exists in more than 10% of drug-treated, but not drug-naïve HIV patients. The connection subdomain mutation N348I has been related to the altered DNA binding affinity and processivity of the mutant enzyme compared to the WT RT (4, 38). Ehteshami et al. showed that N348I enhances resistance to AZT through both RNase H-dependent and -independent mechanisms (10). Since EFdA is a TDRTI and its incorporation is assumed to affect the translocation and thereby DNA binding and processivity, we investigated the susceptibility of two highly potent antiretrovirals EFdA and ENdA.

We report that both EFdA-TP and ENdA-TP are very potent inhibitors of N348I, D67N/K70R/L210Q/T215F, D67N/K70R/L210Q/T215F/N348I, and A62V/V75I/F77L/F116Y/Q151M RTs. They inhibit RT primarily at the point of incorporation and since they prevent enzyme translocation they both belong to the TDRTI class of NRTIs. The D67N/K70R/L210Q/T215F set of mutations are the classical thymidine-associated mutations (TAMs), which are known to cause resistance to AZT by enhancing excision of AZT-terminated primers (1, 5, 23). The A62V/V75I/F77L/F116Y/Q151M set of mutations is known as the "Q151M" complex RT, and has been known as a multidrug-resistance mutation, since the latter mutations are known to be involved in resistant variants with reduced susceptibility to dideoxynucleotides and to AZT. Unlike D67N/K70R/L210Q/T215F RT, the Q151M complex decreases susceptibility to NRTIs by decreasing incorporation efficiency of the inhibitors rather than increasing excision and unblocking of chain-terminated primers (14). Finally, N348I is known to cause resistance to both NRTIs and NNRTIs. Hence, collectively, these mutants represent all mechanisms by which RT becomes resistant to available antivirals. Importantly, we find that they are all susceptible to the EFdA and ENdA TDRTIs.

Hence, this new class of RT inhibitors should be able to efficiently block viruses that carry clinically relevant mutations, including the new connection domain mutation N348I.

ACKNOWLEDGEMENTS

This work was supported by the Ministry of Knowledge and Economy, Bilateral International Collaborative Research and Development Program, Republic of Korea, National Institutes of Health Grants AI076119, AI074389, and AI100890 (to S. G. S.) and AI079801 (to M.A.P.).

Other articles in this theme issue include references (44-71).

REFERENCES

1. Arion, D., N. Kaushik, S. McCormick, G. Borkow, and M. A. Parniak. Phenotypic mechanism of HIV-1 resistance to 3'-azido-3'-deoxythymidine (AZT): increased polymerization processivity and enhanced sensitivity to pyrophosphate of the mutant viral reverse transcriptase. *Biochem.* 1998,**37**:15908-15917.

2. Bauman, J. D., K. Das, W. C. Ho, M. Baweja, D. M. Himmel, A. D. Clark, Jr., D. A. Oren, P. L. Boyer, S. H. Hughes, A. J. Shatkin, and E. Arnold. Crystal engineering of HIV-1 reverse transcriptase for structure-based drug design. *Nucleic Acids Res.* 2008, **36:**5083-5092.

3. Biaglow, J. E., and A. V. Kachur. The generation of hydroxyl radicals in the reaction of molecular oxygen with polyphosphate complexes of ferrous ion. *Radiat Res.* 1997, **148**:181-187.

4. Biondi, M. J., G. L. Beilhartz, S. McCormick, and M. Gotte. N348I in HIV-1 reverse transcriptase can counteract the nevirapine-mediated bias toward RNase H cleavage during plus-strand initiation. *J Biol Chem.*2010, 285 **(35)**:26966-26975.

5. Boyer, P. L., S. G. Sarafianos, E. Arnold, and S. H. Hughes. Selective excision of AZTMP by drug-resistant human immunodeficiency virus reverse transcriptase. *J Virol.* 2001, **75**:4832-4842.

6. Brehm, J. H., D. Koontz, J. D. Meteer, V. Pathak, N. Sluis-Cremer, and J. W. Mellors. Selection of mutations in the connection and RNase H domains of human immunodeficiency virus type 1 reverse transcriptase that increase resistance to 3'-azido-3'-dideoxythymidine. *J Virol.* 2007, **81**:7852-7859.

7. Das, K., J. Ding, Y. Hsiou, A. D. Clark, Jr., H. Moereels, L. Koymans, K. Andries, R. Pauwels, P. A. Janssen, P. L. Boyer, P. Clark, R. H. Smith, Jr., M. B. Kroeger Smith, C. J. Michejda, S. H. Hughes, and E. Arnold. Crystal structures of 8-Cl and 9-Cl TIBO complexed with wild-type HIV-1 RT and 8-Cl TIBO complexed with the Tyr181Cys HIV-1 RT drug-resistant mutant. *J Mol Biol.* 1996, **264**:1085-1100.

8. Delviks-Frankenberry, K. A., G. N. Nikolenko, R. Barr, and V. K. Pathak. Mutations in human immunodeficiency virus type 1 RNase H primer grip enhance 3'-azido-3'-deoxythymidine resistance. *J Virol.* 2007, **81**:6837-6845.

9. Dharmasena, S., Z. Pongracz, E. Arnold, S. G. Sarafianos, and M. A. Parniak. 3'-Azido-3'-deoxythymidine-(5')-tetraphospho-(5')-adenosine, the product of ATP-mediated excision of chain-terminating AZTMP, is a potent chain-terminating substrate for HIV-1 reverse transcriptase. *Biochem.* 2007, **46:**828-836.

10. Ehteshami, M., G. L. Beilhartz, B. J. Scarth, E. P. Tchesnokov, S. McCormick, B. Wynhoven, P. R. Harrigan, and M. Gotte. Connection domain mutations N348I and A360V in HIV-1 reverse transcriptase enhance resistance to 3'-azido-3'-deoxythymidine through both RNase H-dependent and -independent mechanisms. *J. Biol.Chem.* 2008, **283**:22222-22232.

11. Goff, S. P. Retroviral reverse transcriptase: synthesis, structure, and function. *J Acquir Immune Defic Syndr.* 1990, **3**:817-831.

12. Gotte, M., J. W. Rausch, B. Marchand, S. Sarafianos, and S. F. Le Grice. Reverse transcriptase in motion: conformational dynamics of enzyme-substrate interactions. *Biochim Biophys Acta.* 2010, **1804**:1202-1212.

13. Hachiya, A., E. N. Kodama, S. G. Sarafianos, M. M. Schuckmann, Y. Sakagami, M. Matsuoka, M. Takiguchi, H. Gatanaga, and S. Oka. Amino acid mutation N348I in the connection subdomain of human immunodeficiency virus type 1 reverse transcriptase confers multiclass resistance to nucleoside and nonnucleoside reverse transcriptase inhibitors. *J. virol.* 2008, **82**:3261-3270.

14. Hachiya, A., E. N. Kodama, M. M. Schuckmann, K. A. Kirby, E. Michailidis, Y. Sakagami, S. Oka, K. Singh, and S. G. Sarafianos. K70Q adds high-level tenofovir resistance to «Q151M complex» HIV reverse transcriptase through the enhanced discrimination mechanism. *PloS one.* 2011,**6**:e16242.

15. Hachiya, A., K. Shimane, S. G. Sarafianos, E. N. Kodama, Y. Sakagami, F. Negishi, H. Koizumi, H. Gatanaga, M. Matsuoka, M. Takiguchi, and S. Oka. Clinical relevance of substitutions in the connection subdomain and RNase H domain of HIV-1 reverse transcriptase from a cohort of antiretroviral treatment-naive patients. *Antiviral Res.* 2009, **82**:115-121.

16. Jacobo-Molina, A., J. Ding, R. G. Nanni, A. D. Clark, Jr., X. Lu, C. Tantillo, R. L. Williams, G. Kamer, A. L. Ferris and P. Clark. Crystal structure of human immunodeficiency virus type 1 reverse transcriptase complexed with double-stranded DNA at 3.0 A resolution shows bent DNA. *PNAS.* 1993, **90**:6320-6324.

17. Julias, J. G., M. J. McWilliams, S. G. Sarafianos, W. G. Alvord, E. Arnold, and S. H. Hughes. Mutation of amino acids in the connection domain of human immunodeficiency virus type 1 reverse transcriptase that contact the template-primer affects RNase H activity. *J Virol.* 2003, **77**:8548-8554.

18. Kawamoto, A., E. Kodama, S. G. Sarafianos, Y. Sakagami, S. Kohgo, K. Kitano, N. Ashida, Y. Iwai, H. Hayakawa, H. Nakata, H. Mitsuya, E. Arnold, and M. Matsuoka. 2'-deoxy-4'-C-ethynyl-2-halo-adenosines active against drug-resistant human immunodeficiency virus type 1 variants. *Int J Biochem Cell Biol.* 2008, **40**:2410-2420.

19. Kodama, E. I., S. Kohgo, K. Kitano, H. Machida, H. Gatanaga, S. Shigeta, M. Matsuoka, H. Ohrui, and H. Mitsuya. 4'-Ethynyl nucleoside analogs: potent inhibitors of multidrug-resistant human immunodeficiency virus variants in vitro. *Antimicrob Agents Chemother.* 2001, **45**:1539-1546.

20. Kohlstaedt, L. A., J. Wang, J. M. Friedman, P. A. Rice, and T. A. Steitz. Crystal structure at 3.5 A resolution of HIV-1 reverse transcriptase complexed with an inhibitor. *Science.* 1992, **256**:1783-1790.

21. Marchand, B., and M. Gotte. Site-specific footprinting reveals differences in the translocation status of HIV-1 reverse transcriptase. Implications for polymerase translocation and drug resistance. *J Biol Chem.* 2003, **278**:35362-35372.

22. Menendez-Arias, L., and B. Berkhout. Retroviral reverse transcription. *Virus Res.* 2008,**134**:1-3.

23. Meyer, P. R., S. E. Matsuura, A. M. Mian, A. G. So, and W. A. Scott. A mechanism of AZT resistance: an increase in nucleotide-dependent primer unblocking by mutant HIV-1 reverse transcriptase. *Mol Cell.* 1999, **4**:35-43.

24. Meyer, P. R., S. E. Matsuura, A. G. So, and W. A. Scott. Unblocking of chain-terminated primer by HIV-1 reverse transcriptase through a nucleotide-dependent mechanism. *Proc Nat Acad Sci USA.* 1998, **95**:13471-13476.

25. Meyer, P. R., S. E. Matsuura, A. A. Tolun, I. Pfeifer, A. G. So, J. W. Mellors, and W. A. Scott. Effects of specific zidovudine resistance mutations and substrate structure on nucleotide-dependent primer unblocking by human immunodeficiency virus type 1 reverse transcriptase. *Antimicrob Agents Chemother.* 2002, **46**:1540-1545.

26. Michailidis, E., B. Marchand, E. N. Kodama, K. Singh, M. Matsuoka, K. A. Kirby, E. M. Ryan, A. M. Sawani, E. Nagy, N. Ashida, H. Mitsuya, M. A. Parniak, and S. G. Sarafianos. Mechanism of inhibition of HIV-1 reverse transcriptase by 4'-Ethynyl-2-fluoro-2'-deoxyadenosine triphosphate, a translocation-defective reverse transcriptase inhibitor. *J Biol Chem.* 2009, **284**:35681-35691.

27. Nikolenko, G. N., K. A. Delviks-Frankenberry, S. Palmer, F. Maldarelli, M. J. Fivash, Jr., J. M. Coffin, and V. K. Pathak. Mutations in the connection domain of HIV-1 reverse transcriptase increase 3'-azido-3'-deoxythymidine resistance. *Proc Nat Acad Sci USA.* 2007, **104**:317-322.

28. Nikolenko, G. N., K. A. Delviks-Frankenberry, and V. K. Pathak. A novel molecular mechanism of dual resistance to nucleoside and nonnucleoside reverse transcriptase inhibitors. *J Virol.* 2010, **84**:5238-5249.